Department of Biomedical Sciences

University of Veterinary Medicine Vienna

Institute for Medical Biochemistry

(Head: Univ.-Prof. Dr. rer.nat. Florian Grebien)

The Role of the DEAD box RNA helicase DDX6 in normal and malignant hematopoiesis

Master thesis submitted for the fulfillment of the requirements for the degree of

Master of Science (MSc)

University of Veterinary Medicine Vienna

Submitted by

Bernhard Alber, BSc

Vienna, July 2022

Supervisor: Univ.-Prof. Dr.rer.nat Florian Grebien

University of Veterinary Medicine Vienna

Department of Biomedical Science

Institute for Medical Biochemistry

Veterinärplatz 1

1210 Vienna

Reviewer: Karoline Kollmann, PhD

University of Veterinary Medicine Vienna

Department of Biomedical Science

Institute for Pharmacology and Toxicology

Veterinärplatz 1

1210 Vienna

Index

1) Introduction

1.1) Leukemia

Leukemia is a malignant disease of the hematopoietic tissue that affects the bone marrow and the lymphatic system. This disease causes an abnormal proliferation of malignant blood cells. Depending on how quickly the disease progresses we can distinguish between acute and chronic types of leukemia. Acute leukemias are rapidly progressing and more aggressive than chronic forms and result in the accumulation of immature blood cells in the bone marrow. Chronic leukemia's are characterized by delayed disease onset and an accumulation of mature cell types in the bone marrow and blood of patients. Leukemia's can be further distinguished depending on which blood cell type they arise from. Myeloid leukemia's affect the myeloid lineage of hematopoiesis whereas lymphoid leukemia's represent aberrant lymphoid development. Taken together this allows to differentiate between four major classes of leukemia: acute myeloid leukemia, chronic myeloid leukemia, acute lymphoid leukemia and chronic lymphoid leukemia. Overall, leukemia's are rare types of cancer as they only represent 7% of all diagnosed cancers in males and females combined (Siegel et al. 2021).

1.2) Acute Myeloid Leukemia

Acute myeloid leukemia (AML) is a neoplasm of the stem/progenitor cells that are committed to the myeloid lineage (Pelcovits and Niroula 2020). AML is a rare disease, accounting only for a small percentage of newly diagnosed cancer cases each year, although it is the most common form of acute leukemia in adults (De Kouchkovsky and Abdul-Hay 2016). AML is characterized by an accumulation of abnormal white blood cells (so called myeloblasts) in the bone marrow. This leads to the disruption of normal hematopoiesis and to a reduction in healthy blood cells (alfa-leukemia.org), causing fatigue, anemia, anorexia and weight loss (De Kouchkovsky and Abdul-Hay 2016).

There are two classification systems for acute myeloid leukemias. The older French-American-British system is based on the morphology of AML blasts under light microscopy (De Kouchkovsky and Abdul-Hay 2016). As it was developed in the late 1970s, however, this classification system fails to incorporate the advancements made in the recent years. The newer classification system was developed by the WHO and takes different genetic and molecular causes of acute myeloid leukemia and how they affect treatment outcomes and disease progression into consideration (Hwang 2020). The WHO groups AML into six different

categories: AML with recurrent genetic abnormalities; AML with myelodysplasia related changes (MRC); therapy related myeloid neoplasms (t-MN); AML not otherwise specified (NOS); myeloid sarcoma; and myeloid proliferations related to Down Syndrome (DS) (Hwang 2020).

Since AML is a heterogeneous disease, there is no single underlying cause. Common genetic alterations are chromosomal aberrations that result in fusion genes which lead to the expression of oncogenic fusion proteins such as PML-RARα, MLL-AF9 or NUP98-HOXA9 (Martens and Stunnenberg 2010), activating and or point mutations in oncogenes that affect signaling pathways that are critical for normal blood cell development. For example, mutations in *FLT3, KRAS or NRAS* result in dysregulated signaling cascades (DiNardo and Cortes 2016). Mutations in transcription factors and master regulators of myeloid differentiation such as C/EBPα, RUNX1 and GATA2 lead to aberrant gene expression, and mutations in epigenetic regulators like DNMT3A, TET2, ASXL1 and IDH1/IDH2 change patterns of DNA methylation and chromatin modification. Lastly mutations in tumor suppressor genes such as *TP53* are found in AML (DiNardo and Cortes 2016). In general, identifying the underlying mutation in AML patients is essential for finding the right treatment approach for this disease.

1.3) Treatment and targeted therapies in AML

For over 40 years, the standard therapy for AML consisted of the “7+3” regime of chemotherapy. In this treatment approach, Cytarabine is given continuously for seven days with Daunorubicin being administered for the first three days (Kantarjian et al. 2021). Following chemotherapy, patients with a high risk of relapse can undergo hematopoietic stem cell transplantation (Kassim and Savani 2017). However, this treatment approach can be poorly tolerated in older patients and people with significant comorbidities (Daver et al. 2020).

Other treatment options include small molecule inhibitors and/or targeted therapy approaches provide alternatives to the standard “7+3” regime. Targeted therapies aim to combat cancer-specific mutations by selective inhibition of mutated or overexpressed genes. For example, the BCL-2 family of proteins plays an essential role in cell-intrinsic apoptosis (Kale, Osterlund, and Andrews 2018). Overexpression of BCL-2 specifically has been associated with therapy resistance and apoptosis evasion in hematological malignancies (Samra et al. 2020).As a result, the selective BCL-2 inhibitor Venetoclax is already used in clinics to treat AML patients.

A second example of targeted therapy is the small-molecule-mediated inhibition of aberrant FLT3 signaling. FLT3 is a member of the receptor tyrosine kinase family which regulates proliferation through the RAS and ERK signaling pathways, as well as cell survival and transcription of anti-apoptotic genes through PI3K and AKT/mTOR signaling (Grafone et al. 2012). *FLT3* mutations are found in both adult and pediatric AML cases (Smith 2019). Internal tandem duplications (ITD) give rise to the most common *FLT3* mutations in AML (termed FLT3-ITD), while mutations in the tyrosine kinase domain (TKD) lead to FLT3-TKD. Both types of lesions represent important driver mutation in leukemia (Daver et al. 2019). The FLT3 inhibitor Midostaurin is currently used in clinics together with the 7+3 chemotherapeutic regime to treat *FLT3*-mutated AML (Kantarjian et al. 2021; Daver et al. 2019). It has been shown that this combination therapy increases the rates of clinical remissions and short-term survival in multiple clinical studies (Kantarjian et al. 2021).

Mutations in the isocitrate dehydrogenase genes *IDH1* and or *IDH2* occur in 20% of all AML cases (Issa and DiNardo 2021). Most mutations are found in the active site and disrupt the normal enzymatic function of IDH proteins but lead to the production of the oncometabolite 2-hydroxyglutarate (2-HG) (Dang et al. 2009). Elevated levels of 2-HG inhibit the function of TET2 and other epigenetic regulators, producing the characteristic hypermethylation phenotype observed in *IDH1/2* mutated AML (Figueroa et al. 2010). The hypermethylation caused by TET2 inactivation results in an impairment of myeloid differentiation (Figueroa et al. 2010). Targeting mutated IDH1/2 with Ivosidenib and Enasidenib, respectively, has been shown to improve overall remission rates and clinical responses in clinical trials (Issa and DiNardo 2021). Since *IDH1/2* mutations result in a dependency on BCL-2 to prevent apoptosis in leukemia (Chan et al. 2015), the FDA approval of the *IDH1/2* inhibitor Ivosidenib provided an important asset in combating AML with these mutations (Chan et al. 2015).

Another prominent example of targeted therapy in AML is the targeting of the PML-RARA fusion protein in acute promyelocytic leukemia (APL). This fusion protein occurs in 98% of all APL cases (De Braekeleer, Douet-Guilbert, and De Braekeleer 2014). PML has important tumor suppressor functions. It promotes apoptosis and senescence by stabilizing the tumor suppressor p53. In addition, PML induces calcium release from the ER, leading to the activation of p53-independent apoptosis. Furthermore, PML also plays a role in various other forms of induced cellular senescence and apoptosis, such as KRAS-induced senescence and

DNA damage-mediated apoptosis (Hsu and Kao 2018). Finally, PML negatively regulates tumor angiogenesis (Hsu and Kao 2018). Through its interaction with numerous partner proteins, PML can also be involved in many different pathways such as stem cell self-renewal (Ito et al. 2012), epigenetic regulation (Yoshida et al. 2007) and transcriptional regulation of hematopoietic stem cell function (Wang et al. 2018). In contrast. The activity of RARA activity strongly depends on the presence of ligands such as ATRA, LXRα, NFκB-1, insulin growth factor binding protein (IGFBP) 3 and importin β (Dawson and Xia 2012; Xu et al. 2020). In the presence of ligands RARA acts as a transcription factor, whereas the absence of ligands causes RARA to act as a transcriptional repressor (Liquori et al. 2020). PML-RARA fusion protein acts in two ways. On the one hand it blocks transcription of several genes that are important for myeloid differentiation (Gaillard et al. 2015). On the other hand, it provides leukemia cells with a competitive advantage over normal hematopoietic cells (Kamashev, Vitoux, and De The 2004). The common treatment for *PML-RARA*-mutated APL is the administration of all trans retinoic acid and arsenic trioxide. Retinoic acid binds the fusion protein through interaction with the ligand binding domain of RARA, inducing a conformational change and activating the transcription of target genes. This induces proteasomal degradation of the fusion protein and causes APL cells to terminally differentiate. Arsenic trioxide targets the PML domain of the PML-RARA fusion protein and induces apoptosis via the sumoylation of the fusion protein (Nasr et al. 2009).Treatment with these agents has increased the overall remission rate of APL to 95% and the cure rates up to 80% (Lo-Coco et al. 2013).

1.4) Cancer genetic dependencies

For a cancer to form, multiple genetic and/or epigenetic changes are required. The difference between driver and passenger mutations is essential to discovering cancer-specific genetic dependencies. A driver mutation confers a selective growth advantage to cancer cells, whereas passenger mutations are acquired over time due to the inherent genetic instability of cancers. Genetic dependencies of any cancer are defined as genes that are selectively essential for cancer cells proliferation and survival (Lin and Sheltzer 2020). Scientists try to discover cancer genetic dependencies as potential therapeutic targets. The best example for this is the BCR-ABL fusion kinase, which is generated by the t(9;22) chromosomal translocation and is characteristic for chronic myeloid leukemia (CML) (Ben-Neriah et al. 1986). CML is now commonly treated with the tyrosine kinase inhibitor Imatinib which blocks ATP binding to the inactive form of the ABL kinase preventing its switch to an active conformation

(An et al. 2010). Treatment with Imatinib results in a complete cytogenetic response in 89% of all CML patients (Iqbal and Iqbal 2014). Mouse models for HRAS-dependent melanomas are another example of genetic dependency or oncogene addiction. The inactivation of RAS oncogene led to tumor cell apoptosis (Sharma and Settleman 2007) (Sharma and Settleman 2007). The recent FDA approval of the specific KRAS inhibitor Sotorasib enabled the development of targeted therapies against cancers with a genetic dependency on KRAS. Some genes may be genetic dependencies in multiple cancers whereas others are highly specific for particular cancer types. HER2, a member of the receptor tyrosine kinase family is essential for cancer cell growth in breast cancer harboring an *EFGR* mutation or amplification and its inhibition in tumors that are driven by this mutation leads to cell death. However, in breast cancer that is driven by mutations in the estrogen receptor the blockage of HER2 with trastuzumab-based chemotherapy has little to no effect on patient outcome (Paplomata, Nahta, and O'Regan 2015).

To discover genetic dependencies in cancer, scientists have an array of tools at their disposal. For example, the RNA interference (RNAi) technique takes advantage of endogenous RNA silencing pathways to achieve the knockdown of any gene of interest at the post-transcriptional level, resulting in decreased protein expression (Agrawal et al. 2003). Through the use of RNAi-induced gene knockdowns it became possible to study the effects of loss of any protein of interest on cancer cells. This has enabled scientists to discover proteins that are selectively essential for cancer cell survival and are therefore genetic dependencies of particular cancer types (Boutros and Ahringer 2008). Besides the RNAi system, the clustered regularly interspaced short palindromic repeats (CRISPR) Cas9 system has emerged as a powerful tool for the identification of cancer-specific dependencies. In this system the Cas9 endonuclease can be guided to any gene in the genome by the use of complementary single guide RNAs (sgRNAs). There, the Cas9 enzyme induces double strand breaks, which are repaired through an error prone DNA repair system. This process introduces insertion or deletion (indel) mutations. In turn, such indels can lead to frame-shift mutations and/or affect protein translation and thereby can disrupt gene function (Doudna and Charpentier 2014). Based on that, the CRISPR/Cas9 technology has the potential to overcome some limitations that are linked to the RNAi system. The usage of the protospacer adjacent motif (PAM), a short conserved 2-5 base pair motif that is located next to the target DNA and necessary to distinguish between self and non-self (Gleditzsch et al. 2019). The design of highly specific sgRNAs allow researchers to

induce CRISPR/Cas9-induced gene knockouts with high precision. This is superior to RNAi mediated gene knockdown, which is prone to off target effects. As in the RNAi system, the target mRNA is down-regulated but not eradicated, inefficient gene knockdown can result in residual mRNA expression as well as off-target effects. Thus, RNAi may not be sufficient to achieve a loss-of-function phenotype (Boettcher and McManus 2015). However also CRISPR Cas9 has its disadvantages. The mutations caused are irreversible since they are introduced by the cells own DNA damage repair system. Furthermore, the complete loss of gene function may result in the absence of effects that are only observable under lower protein concentrations cause by gene knockdown. Both RNAi and CRISPR/Cas9 approaches can be applied for genome wide screening, with the latter providing a higher sensitivity and limited off-target effects. Irrespective of whether the RNAi or CRISPR/Cas9 approach is used, genome wide screens work by introducing a library of sequences (siRNAs, shRNAs or sgRNAs) which target every gene in the genome into a population of cells. Cellular proliferation is then followed over a distinct period. During this process, some sequences will be lost due to the disruption of essential gene functions and the resulting death of affected cells. At the end point of the screen genomic DNA is isolated and shRNA/sgRNA sequences are analyzed by next generation sequencing. The abundance of reads for every shRNA/sgRNA at the endpoint of the screen are compared to their abundance in the initial sequence pool. The absence of a sequence in the endpoint sample but its presence in the initial sequence pool indicates that this particular sgRNA sequence led to the disruption of a gene which is essential for cellular proliferation, as cells expressing this sequence were lost during the experiment. This makes genome-wide screens a powerful tool to study and discover potential cancer specific genetic dependencies. An example of the efficiency of CRISPR/Cas9 screens in the identification of cancer specific dependencies is the discovery of the RNA-binding protein Staufen2 as an important regulator of myeloid leukemia (Bajaj et al. 2020),

The Cancer Dependency Map (DepMap) database is a useful resource to mine cancer genetic dependencies from a high number of genome-wide CRISPR/Cas9 screens in human cancer cell lines (Pacini et al. 2021). These datasets provide important information on cancer-specific dependencies and aid scientists in developing new targeted therapies.

1.5) RNA-binding proteins (RBPs) in AML

RNA metabolism plays an important role in regulating cell differentiation and proliferation (Fraga de Andrade, Mehta, and Bresnick 2020; Corsini et al. 2018; Cesana et al. 2011; Mazzoni and Falcone 2011). RNAs are frequently bound by proteins as well as other coding and non-coding RNAs to give rise to ribonucleoprotein complexes (RNPs) (Pereira, Billaud, and Almeida 2017). RNA binding proteins (RBPs) are important for nearly all post-transcriptional processes including splicing, alternative polyadenylation, localization, surveillance, decay and translation (Kim, Hur, and Jeong 2009; Kang, Lee, and Lee 2020). RBPs can bind to either unstructured regions within the untranslated regions or within the open reading frame of target mRNAs (Wurth 2012). They utilize so-called RNA recognition motifs to achieve this binding. Some well-characterized RNA recognition motifs include the K-Homology domain, the double stranded RNA binding motif, the RGG (Arg-Gly-Gly) box or the DEAD/DEAH (Asp-Glu-Ala-Asp)/ (Asp-Glue-Ala-His) box motif (Kim, Hur, and Jeong 2009). The interaction of RNAs with RBPs creates a platform to attract and bind more RBPs, generating a hub that controls the fate of the bound mRNA (Kim, Hur, and Jeong 2009).

The dysregulation of this complex network of RNA-protein interactions has been proposed to play a role in many diseases, including cancer (Lukong et al. 2008). It has been reported that RNA-binding proteins are aberrantly expressed in cancer tissues in comparison to their surroundings (King et al. 2011; Vo et al. 2012; Hopkins et al. 2016). Since RBPs play a role in many different cellular pathways, even small changes in their expression levels can have large impacts on RNA metabolism and translation (Pereira, Billaud, and Almeida 2017). Alternative splicing is one of the consequences of altered functions of RNA-binding proteins (Fu and Ares 2014). An alternative splicing program leads to the expression of different protein isoforms, which can result in the expression of oncogenes (Pereira, Billaud, and Almeida 2017). Alternatively, altered RBP function can promote cancer by leading to changes in mRNA stability and decay (Benjamin and Moroni 2007). Oncogenes, growth factors and their respective receptors as well as important cell cycle genes are frequently overexpressed in cancer, pointing to an important role of mRNA stability in tumor formation and progression (Benjamin and Moroni 2007).

Translation of nearly all mRNAs is controlled at the step of initiation. RNA-binding proteins play an essential role in this process, as they induce mRNA circularization and mediate ribosomal

loading (Pereira, Billaud, and Almeida 2017). Dysregulated RNA-binding proteins such as Sma68 cause a shift in the balance of pro- and anti-apoptotic proteins by alternative splicing, resulting in the inhibition of apoptosis in cancer cells (Paronetto et al. 2007). Also, RBPs play important roles in more than one hallmark of cancer and they act as amplifiers of oncogenic driver mutations by affecting cancer-associated downstream targets following the initial mutation (Pereira, Billaud, and Almeida 2017). Figure 1 shows an overview of the post-transcriptional mechanisms that involve RNA-binding proteins in cancer.

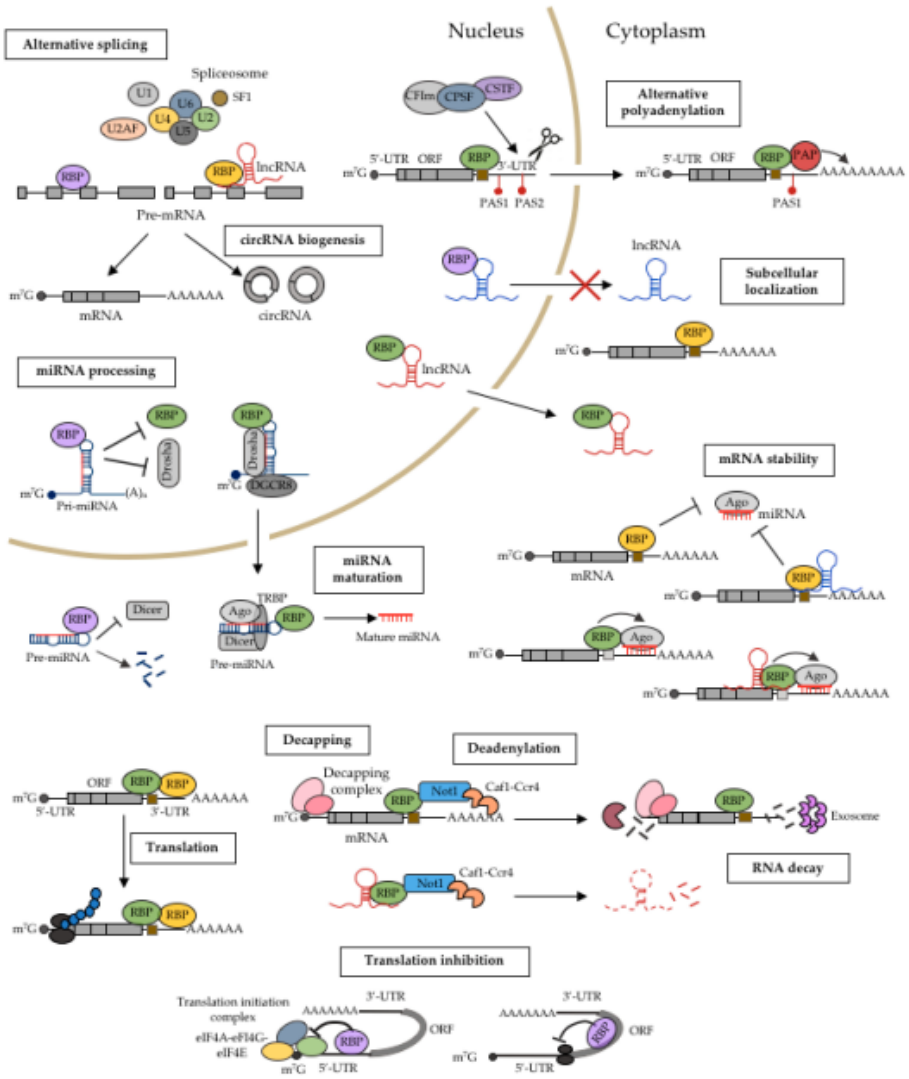

Figure 1: Mechanistic role of RNA-binding proteins in the post-transcriptional regulation of gene expression (Kang, Lee, and Lee 2020).

RNA-binding proteins are often aberrantly expressed in AML cell lines and patient samples (Wang et al. 2019). A genome wide CRISPR screen performed by Bajaj et. al showed that RNA binding proteins are frequent genetic dependencies in leukemia (Bajaj et al. 2020). The change in expression of RBPs leads to a disruption of the fine-tuned network of post-transcriptional regulation of gene expression. For example, RBM39 is an RBP that is frequently overexpressed in AML (Wang et al. 2019). RBM39 overexpression leads to aberrant splicing of the *HOXA9* target gene to promote leukemia cell survival (Wang et al. 2019). Another RNA binding protein frequently overexpressed in AML is Musashi 2 (MSI2) (Schuschel et al. 2020) which has been described as a genetic dependency in several leukemia subtypes, including *CEPBA*-mutated AML (Heyes et al. 2021). MSI2 controls many different intracellular signaling pathways, as it inhibits Notch signaling via regulation of *NUMB* mRNA translation (Kharas et al. 2010). Furthermore, it controls the mitogen-activated protein kinase (MAPK) pathway, which is an important driver of proliferation (McCubrey et al. 2007). Knockdown of *MSI2* caused an increase in apoptosis via the upregulation of *Bax* expression (Han et al. 2015). A recent study showed that a small molecular inhibitor against Musashi 2 is capable of selectively reducing leukemia burden in vivo by selectively inhibiting the oncogenic RNA-binding activity of *MSI2* (Minuesa et al. 2019*)*. The MSI2-interaction partner SYNCRIP is involved in exosomal microRNA sorting and has been shown to be essential in AML by regulating the myeloid leukemia self-renewal post-transcriptional program (Vu et al. 2017). The RNA binding protein RBMX is a tumor suppressor in many different solid cancers. In leukemia however, RBMX acts as a regulator of chromatin compaction and transcriptional activity by binding to the intronic regulator element of *CBX5*. It was shown that RBMX is needed to maintain the leukemic phenotype in vivo and in vitro (Prieto et al. 2021). Another RNA binding protein, RBM17 has been found to be expressed at high levels in human AML stem and progenitor cells. This leads to an escape from the nonsense-mediated decay pathway, causing the stabilization and increased levels of proteins that drive leukemic progression, such as EZH2 and RBM39 (Liu et al. 2022). Nucleolin is an RNA binding protein mainly found in the nucleus, where it interacts with ribosomal DNA and is involved in ribosomal synthesis (Tajrishi, Tuteja, and Tuteja 2011). In AML, nucleolin serves as a diagnostic marker as its overexpression has been associated with poor prognosis, especially in elder patients (Marcel et al. 2017). The overexpression of Nucleolin leads to increased phosphorylation of nuclear factor kappa B, resulting in increased expression of DNA methyltransferase 1 (DNMT1). Overexpressed DNMT1 subsequently

causes DNA hypermethylation resulting in gene expression changes in acute myeloid leukemia (Shen et al. 2014). Thus, given their important roles in disease biology, therapeutic targeting of dysregulated RNA binding proteins appears to be a promising approach for finding novel treatment options for AML.

1.6) Processing bodies

Processing bodies (P-bodies) are membraneless cytoplasmic foci containing mRNPs that are associated with translational repression and mRNA decay machineries (Parker and Sheth 2007). P-body components are broadly associated with RNA metabolism and fall into one of the following categories (Standart and Weil 2018): mRNA decay, translational control and RNA interference. Among those we find DCP1/2 and XRN1, which are involved in the 5' – 3' mRNA degradation pathway (van Dijk et al. 2002), the decapping activators EDC3 and EDC4 (Ling et al. 2008), the mRNA deadenylation factors CCR4 and PAN3 (Zheng et al. 2008), the miRNA-mediated silencing factors AGO1-4 and GW182 (Azuma-Mukai et al. 2008) and proteins with functions in the translation repression pathway such as DDX6, eIF4E and its binding protein 4E-T (Andrei et al. 2005; Ayache et al. 2015). P-bodies assemble through a process called liquid-liquid phase transition. Once a critical concentration of RNA and proteins is reached, this process allows the condensation of components into viscous droplets in the cytoplasm (Hyman, Weber, and Julicher 2014; Sfakianos, Whitmarsh, and Ashe 2016). Only three proteins are essential for the assembly of P-bodies: DDX6, 4E-T and LSM14A (Ayache et al. 2015).

For a long time, the function of P-bodies was thought to be linked to mRNA decay, since the first proteins identified in P-bodies were part of the 5'-3' mediated mRNA decay pathway (Sheth and Parker 2003). Further work provided experimental proof that mRNA decay indeed happens in P-bodies (Sheth and Parker 2003; Cougot, Babajko, and Seraphin 2004). Nevertheless, other studies showed evidence that the mRNAs localizing to P-bodies could re-enter translation (Aizer et al. 2014). These findings led to the development of a model in which untranslated mRNAs are targeted to P-bodies for either mRNA decay or storage (Eulalio, Behm-Ansmant, and Izaurralde 2007). The purification of P-bodies by Hubstenberger et al provided further information on their protein and RNA content (Hubstenberger et al. 2017). They showed that mRNA decay intermediates were absent in P-bodies. Furthermore, upon disruption of P-bodies by depletion of DDX6, no changes in cellular mRNA decay were

observed (Hubstenberger et al. 2017). Taken together, these findings suggest a role for P-bodies in mRNA storage rather than decay.

Analysis of mRNAs enriched in P-bodies showed that they belong to a specific set of regulators of cellular functions, such as mRNA metabolism, cell cycle control, protein catabolism and energy metabolism (Hubstenberger et al. 2017). These findings support a model in which important mRNAs are stored within P-bodies to enable a rapid response to changes in the cellular microenvironment.

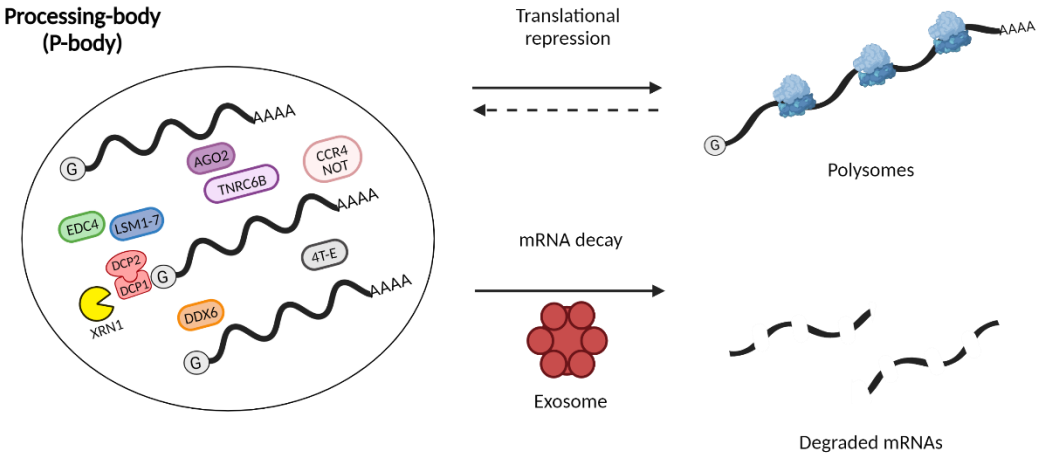

Figure 2: Graphical depiction of P-body function. Image created with Biorender.com

1.7) DEAD-box RNA helicase 6 (DDX6)

Members of the DEAD-box RNA helicases (DDX) partake in nearly every aspect of RNA biology. This includes RNA storage and decay, transcription, translation, miRNA processing, RNA export from the nucleus. In addition, they act as scaffolds for the formation of ribonucleoprotein particles (Rocak and Linder 2004; Linder and Jankowsky 2011).

DEAD-box RNA helicases are a family of enzymes that use ATP to bind to or remodel RNA and RNA-protein complexes (Linder and Jankowsky 2011). The name DEAD-box RNA helicase comes from the conserved sequence motif of aspartic acid, glutamic acid, alanine, aspartic acid (DEAD) residues which is part of the helicase binding domain (Linder and Jankowsky 2011). C-terminal and N-terminal domains flanking the helicase core of DEAD-box proteins mediate the interaction with RNAs or other protein targets (Linder and Jankowsky 2011; Taschuk and Cherry 2020). The enormous diversity of these additional domains allows DEAD-box RNA helicases to participate in every step of cellular RNA metabolism (Taschuk and Cherry 2020)

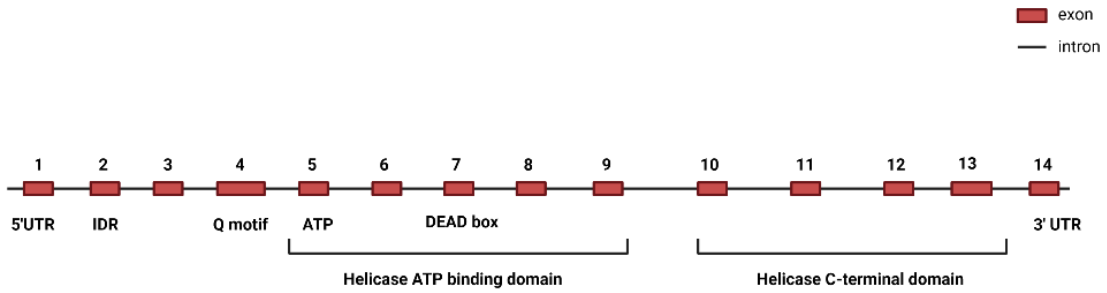

Figure 3) Sequence overview of the DEAD box RNA helicase mRNA

DEAD-box RNA helicases are not only involved in every step of RNA biology (Rocak and Linder 2004) but they also play a crucial role in innate immune sensing. They are part of the canonical cytoplasmic sensor complexes for bacterial DNA and viral DNA/RNA and thus play roles in stimulating the interferon response upon viral infection (Taschuk and Cherry 2020). However, some members of the DEAD-box family can also act as negative regulators of the innate immune response via competition for RNA substrates or protein-protein interactions (Taschuk and Cherry 2020). For example, DDX24 binds to dsRNA and ssRNA and thus interferes with interferon signaling (Ma et al. 2013). DEAD-box RNA helicases can promote or even be essential for efficient viral infections such as DDX5, DDX6 and DDX17.(Bortz et al. 2011; Jangra, Yi, and Lemon 2010; Lorgeoux et al. 2013). DDX3 is member of the DEAD-box RNA helicase family that has been shown to play a role in cancer. In androgen receptor-driven prostate cancer, DDX3 has been reported to cause a downregulation of androgen receptor protein levels, resulting in therapeutic failure (Vellky et al. 2020). Small molecular inhibitors of DDX3 have been generated, and clinical testing is currently underway to determine the effect of DDX3 inhibition as a cancer treatment option (Bol, Xie, and Raman 2015).

DDX6 is another member of the DEAD-box RNA helicase family (Fig 3), which has been shown to have both pro- and antiviral roles. On one hand DDX6 binds to both RIG-I and influenza virus RNA in infected cells to enhance RIG-I signaling and drive the antiviral response (Nunez et al. 2018). On the other hand, depletion of DDX6 induces innate immune signaling pathways that prime cells towards a state of higher responsiveness to interferon signaling (Lumb et al. 2017). Several viruses, including dengue fever virus, are able to hijack P-body components such as DDX6 to aid in the replication of their genome (Ward et al. 2011). DDX6 also plays a role in cancer as it has been shown that DDX6 is highly upregulated in gastric cancer cells. In this context, DDX6 acts as pro-tumorigenic factor because of its interaction with *c-Myc*, leading to an increase in *c-Myc* transcription or the stabilization of *c-Myc* mRNAs. The authors also reported that silencing of DDX6 led to growth inhibition in their model due to the suppression of *c-Myc* expression (Taniguchi et al. 2018).

It has been shown that DDX6 controls mammalian progenitor cell function through selective translation and/or degradation of proliferation-, self-renewal- and differentiation-inducing mRNAs (Wang et al. 2015). Thus, DDX6 is able to control cell fate and differentiation in a context-dependent manner. In adult progenitor cell types, such as neural and endodermal progenitors, DDX6 drives exit from self-renewal towards differentiation (Di Stefano et al. 2019). Conversely, DDX6 maintains self-renewal and inhibits differentiation in mesenchymal and muscle progenitors (Di Stefano et al. 2019). It was also shown that P-bodies and DDX6 mediate the repression of differentiation-inducing genes to maintain intestinal stem cell identity in *Droshophila melanogaster* (Buddika et al. 2022). DDX6 is also involved in the generation of induced pluripotent stem (iPS) cells, as its depletion led to an abrogation of this process (Kami et al. 2018). Nicklas et al. showed that DDX6 increases the activity of the microRNA let-7a in neuronal stem cells, resulting in the induction of neuronal differentiation (Nicklas et al. 2015).

Taken together, these findings point to a dual role of DDX6. Depending on the context and on the specific cell type, DDX6 can promote differentiation at the expense of proliferation and self-renewal or vice versa. The role of DDX6 in normal and malignant hematopoiesis has not been elucidated yet. Indeed, it remains to be discovered whether DDX6 plays a role in maintaining the self-renewal program of AML blasts or if it drives the differentiation towards mature myeloid cells. In this work, we aimed to unravel the role DDX6 in normal and malignant hematopoiesis using CRISPR/Cas9 and RNA interference approaches.

2) Material and Methods

2.1) Cell culture

Stable-Cas9 expressing clones of MV4:11, MOLM13, HL60 and THP1 cells were cultured in RPMI-1640 medium (Gibco, California USA) supplemented with 10% FBS (Cytivia Lifescience, Massachusetts USA), 1% Penicillin/Streptomycin (Thermofisher, Massachusetts USA) and 2% L-Glutamine (Gibco, California USA). KO52 cells stably expressing Cas9 and the Lenti-X 293T cells for viral production were cultured in DMEM medium (Gibco, California USA) supplemented with 10% FBS (Cytivia Lifescience, Massachusetts USA), 1% Penicillin/Streptomycin (Gibco, California USA) and 4% L-Glutamine (Gibco, California USA). Murine hematopoietic progenitor HPC-7 cells stably expressing Cas9 were cultured in IMDM medium (Gibco, California USA) supplemented with 5% FBS (Cytivia Lifescience, Massachusetts USA), 1% Penicillin/Streptomycin (Gibco, California USA), 2% L-Glutamine (Gibco, California USA), 1-thioglycerol and murine stem cell factor (mSCF) at a dilution ratio of 1:50. CNC cells are a murine hematopoietic stem and progenitor cell line harboring N-terminal and C-terminal CEBPA mutations that was previously generated in the group. stably expressing Cas9 CNC cells were cultured in RPMI-1640 (Gibco, California USA) supplemented with 10% FBS (Cytivia Lifescience, Massachusetts USA), 1% Penicillin/Streptomycin (Gibco, California USA), 2% L-Glutamine (Gibco, California USA)., murine interleukin-6 (mIL-6) (10ng/µl), murine interleukin-3 (mIL-3) (5ng/µl) and mSCF at a dilution ratio of 1:50. All cells were kept in a 95% air humidified atmosphere with 5% CO_2 at 37°C in an incubator.

2.2) sgRNA cloning

The lentiviral expression vector pLenti-hU6-sgRNA-IRFP670 was digested for 2 hours at 55°C using the restriction enzyme BsmBI-v2 (New England Biolabs, Massachusetts USA). Following the digestion, the ends of the digested vector were dephosphorylated with 5000 U/ml Antarctic Phosphatase (New England Biolabs, Massachusetts USA) for 1 hour at 37°C. Subsequently, the digested backbone was loaded onto a 0.7% agarose gel, ran for 45 minutes at 110V and gel purified using the MiniPex 3 in 1 Kit (Institute of Molecular Pathology, Vienna Austria).

To phosphorylate and anneal each pair of oligonucleotides,1µl the corresponding forward and reverse oligonucleotides each were mixed with 10x T4 ligation buffer supplemented with 10mM ATP (New England Biolabs, Massachusetts USA) and T4 Polynucleotide Kinase (New

Englands Biolabs, Massachusetts USA). The reaction was incubated in a thermocycler for 30 minutes at 37°C. The annealed oligos were subsequently diluted 1:200 with double distilled water.

For the ligation, 50ng of BsmBI-v2 digested backbone was mixed with the diluted oligonucleotides, T4 ligase Buffer, T4 DNA ligase (both New England Biolabs, Massachusetts USA) and water in a 10 µl reaction. The reaction was incubated for 10 minutes at room temperature. The ligation reaction was subsequently transformed into NEB Stbl3 bacteria as follows: 2 µl of ligation reaction were added to 15 µl bacteria and the mixture was kept on ice for 10 minutes and heat shocked at 42°C for 45 seconds, followed by 2 minutes on ice. Then, 200 µl of LB medium (Carl Roth, Karlsruhe Germany) were added and cells were allowed to recover at 37°C shaking at 700rpm in a thermomixer for 30 minutes. After the recovery, the bacteria were seeded on LB-agar plates containing 100 µg/ml carbenicillin and incubated at 37°C overnight. On the next day single colonies were picked and incubated in 2 ml LB medium supplemented with 100mg/ml carbenicillin overnight at 37°C. The following day the plasmid DNA was isolated using the MiniPex 3 in 1 Kit (Institute of Molecular Pathology, Vienna Austria). Subsequently plasmid DNA was analyzed by Sanger sequencing (Microsynth, Vienna Austria) for confirmation.

sgRNA	**Forward Oligo**	**Reverse Oligo**
sgDDX6 #1_h	caccGATCCAGGATTCTCCCAG	aaacCTGGGAGAATCCTGGATc
sgDDX6#2_h	caccGTACCAGTGCAAACAAGATTG	aaacCAATCTTGTTTGCACTGGTAc
sgDDX6#3_h	caccGAACTTCTGTACACTAAGA	aaacTCTTAGTGTACAGAAGTTc
sgDDX6#4_h	caccGCCAAGAAGATTTCTCAACT	aaacAGTTGAGAAATCTTCTTGGc
sgAgo2 #1_m	caccGAGCGTGTGCAGCGCACGT	aaacACGTGCGCTGCACACGCTc
sgAgo2 #2_m	caccGAAGAAGGAACGGCCAACAG	aaacCTGTTGGCCGTTCCTTCTTc
sgDDX6_15_m	caccGGATCTCATCAAGAAAGGCG	aaacCGCCTTTCTTGATGAGATCC
sgDDX6_11_m	caccGTAAATTGGTTCCTCCGG	aaacCCGGAGGAACCAATTTAC
Caprin1_17_m	caccGTTTGCAAAGGAATTACAG	aaacCTGTAATTCCTTTGCAAAC
Caprin1_7_m	caccGTTGTGTGAGGAGGAAGAGG	aaacCCTCTTCCTCCTCACACAAC
Polr2d_2fillup_m	caccGAAGCGGGCCGTGTAGTTGA	aaacTCAACTACACGGCCCGCTTC
Polr2d_3fillup_m	caccGAAGCGGGCCGTGTAGTTG	aaacCAACTACACGGCCCGCTTC

Table 1: Forward and Reverse oligonucleotides for sgRNA cloning

2.3) shRNA cloning

For the cloning of shRNAs, 5µg of either plasmid backbone capable of expressing the designated insert constitutively or under the control of a doxycycline inducible promoter system were digested using the restriction enzymes XhoI and EcoRI-HF (New England Biolabs, Massachusetts USA) for 2 hours at 37°C. The backbones contained a carbenicillin resistance gene as a selection marker and shRNA expression was coupled to iRFP670. Digested backbones were dephosphorylated using Antarctic Phosphatase (New England Biolabs, Massachusetts USA) for 1 hour at 37°C. Mixtures were loaded on a 0.7% agarose gel and ran for 45 minutes at 110 V. The vectors linearized with XhoI-EcoRI were gel purified using the MiniPex 3 in 1 Kit (Institute of Molecular Pathology, Vienna Austria). DNA concentration was measured at the Spark Tecan Spectrophotometer.

0.05 ng of shRNA oligonucleotides were PCR amplified with 0.5µM mirF forward and reverse primers using Phusion MM polymerase (New England Biolabs, Massachusetts USA). The PCR program used was 5 minutes at 95°C, 25 seconds at 95°C, 25 seconds at 62°C followed by 30 seconds at 72°C. The last three steps were repeated for 30 cycles. After 30 cycles the samples was kept at 72°C for 5 minutes. Following the PCR reaction, the DNA was purified using the MiniPex 3 in 1 Kit (Institute of Molecular Pathology, Vienna Austria).

The purified PCR products were then digested using the restriction enzymes XhoI and EcoRI-HF (New England Biolabs, Massachusetts USA) for 3 hours at 37°C. Following the digestion, fragments were loaded onto a 2% Agarose Gel, run for 45 minutes at 110 V and subsequently gel extracted and purified using the MiniPex 3 in 1 Kit (Institute of Molecular Pathology, Vienna Austria).

For ligation reactions, 300ng of either digested backbone were mixed with 10ng of designated shRNA and T4 DNA Ligase (New England Biolabs, Massachusetts USA) and incubated for 15 minutes at room temperature. Transformation into NEB Stbl3 bacteria was performed as previously described. Following the transformation, the bacteria were plated onto an LB+agar plate containing carbenicillin and incubated at 37°C overnight. The next day single colonies were picked and inoculated into 2 ml of LB supplemented with 100 mg/ml carbenicillin. The inoculated media was placed back into the 37°C incubator overnight. The next day, DNA isolation using the MiniPex 3 in 1 Kit (Institute of Molecular Pathology, Vienna Austria) was

performed as previously described. Subsequently plasmid DNA was analyzed by Sanger sequencing (Microsynth, Vienna Austria) for confirmation.

Name	Sequence
mirF forward oligo	AAACAAGATAATTGCTCGAATTCTAGCCCCTTGAAGTCCGAGGCAGTAGGCA
mirF reverse oligo	TAACCCAACAGAAGGCTCGAGAAGGTATATTGCTGTTGGCAGTGAGCG
Human shDDX6 #1	TGCTGTTGACAGTGAGCGCCCAGATGATAGTATTGGATGATAGTGAAGCCACA GATGTATCATCCAATACTATCATCTGGATGCCTACTGCCTCGGA
Human & Mouse shDDX6 #2	TGCTGTTGACAGTGAGCGCCCAAAGGATCTAAGAATCAAATAGTGAAGC CACAGATGTATTTGATTCTTAGATCCTTTGGATGCCTACTGCCTCGGA
Human shDDX6 #3	TGCTGTTGACAGTGAGCGCACCCGAGGTATTGATATACAATAGTGA AGCCACAGATGTATTGTATATCAATACCTCGGGTATGCCTACTGCCTCGGA
Mouse shDDX6 #1	TGCTGTTGACAGTGAGCGCCCAGATGATAGTGCTAGATGATAGTGAAGCCACAG ATGTATCATCTAGCACTATCATCTGGATGCCTACTGCCTCGGA
Mouse shDDX6 #3	TGCTGTTGACAGTGAGCGCAGCCATCAACTTGATCACTTATAGTGAAGC CACAGATGTATAAGTGATCAAGTTGATGGCTATGCCTACTGCCTCGGA

Table 2: Sequences for the mirF forward and reverse oligonucleotides used for the PCR, sequences of the different shRNAs whereas mouse and human shRNA#2 have the same sequence

2.4) Virus production and viral transduction

HEK-293-derived LentiX cells were seeded in a 6-well plate in the morning and used for transfections 6-8 hours later. 346ng of psPAX2 (containing gag, pro and pol) were mixed with 173ng of the VSV-G envelope expressing plasmid pMD2.G in DMEM (Gibco, California USA). Subsequently, 690ng of the desired constructs were added. 3.6 µl of the Polycationic substance polyethylenimine (PEI) was added to condense the DNA into positively charged particles. Following the addition of PEI this mixture was vortexed, spun down and incubated at room temperature for 20 minutes. Then it was added to the LentiX cells in a dropwise manner to ensure equal distribution of viral particles. On the next day, the media was removed from the cells and replaced with RPMI-1640 (Gibco, California USA) supplemented with 10% FBS (Cytivia Lifescience, Massachusetts USA), 1% Penicillin/Streptomycin (Gibco, California USA)

and 2% L-Glutamine (Gibco, California USA). Lentiviral supernatants were collected 48 and 72 hours after transfection, filtered through 0,45 µm filters and stored at 4°C. Whenever the virus production was performed in a 10cm dish format, 2µg of psPAX2 and 1µg of pMD2.G was used and the amount of the desired viral expression construct was increased to 4µg.

For lentiviral infections human and murine AML cells were either seeded in a 24 well plate at a density of $0.5x10^6$ cells per well or in a 6 well plate at a density of $2x10^6$ cells per well. The cells were counted, spun down and the conditioned media was collected and stored for later use. The cells were resuspended in fresh media and 10 ng/ml Polybrene (Merck, Massachusetts USA) was added to enhance the transfection. Supernatants from virus-producing cells was either added at a concentration of 1:4 or 1:8. Spinfections were performed for 90 minutes at 900g. The following day, the media was removed and replaced with a 1:1 mixture of fresh media and conditioned media for each cell line.

2.5) Competition based proliferation assay

To assess the effect of gene knockout/knockdown on cell proliferation cells were seeded at a density of either $0,5x10^6$ or $1x10^6$ cells per well in a 24 well format. Both, the expression of sgRNAs and shRNAs are linked to iRFP670 so that their expression can be measured by the presence of the iRFP670 signal. We were using lentiviral titers that allow the infection of 30-60% of cells in the population. Therefore, competition-based proliferation assay can be initiated from a pool of transduced and non-transduced cells, and it is possible to monitor the growth competition between cells that were transduced with our constructs and non-transduced cells. The levels of iRFP670-positive cells were measured at regular intervals by flow cytometry using the IntelliCyt iQue Screener Plus (Sartorius, Göttingen Germany). Values of iRFP670-positive cells were normalized either to day 3 or day 5 post lentiviral transduction.

2.6) RNA isolation and qPCR

Cells were pelleted and snap frozen in liquid nitrogen and stored at -80°C unless used immediately. RNA extraction was performed using the NEB Monarch Total RNA Miniprep Kit according to the manufacturer's protocol (New England Biolabs, Massachusetts USA). RNA concentration was measured at the Tecan Spark Spectrophotometer.

500 ng of RNA were used as input for cDNA conversion using the RevertAid First Strand cDNA Synthesis Kit (Thermofisher, Massachusetts USA) according to the manufacturer's instructions.

qPCR was performed in triplicates for each sample in a 96-well format. Forward and reverse primers (10 µM each) were added to the respective wells. A master mix containing cDNA, water and SsoAdvanced Universal SYBR Green Supermix (Bio Rad, California USA) was added and PCR reactions were run on a Bio-Rad CFX96-Real Time PCR detection system. Absolute gene expression was determined by calculating the percentage of gene expression relative to GAPDH using the formula $2^{(-\Delta C(t))} * 100$.

Name	Sequence
GAPDH forward primer	TGCACCACCAACTGCTTAGC
GAPDH reverse primer	GGCATGGACTGTGGTCATGAG
DDX6 mouse forward primer	AATAAAGGACCGAGGGTGCGG
DDX6 mouse reverse primer	ACTCACTTCAATCCCACGCC
DDX6 human forward primer	GGCAGCGGAGGAGATTGACG
DDX6 human reverse primer	GCAATGCAGGCAAGCACCTG

Table 3: Primers with their sequences used in the qPCR quantification

2.7) Western Blot

Cells were pelleted by collecting 3 ml of cell suspension and subsequent centrifugation for 5 minutes at 300g. The cells were then washed once with PBS and pelleted again at 300g for 5 minutes at 4°C. Cell pellets were snap frozen in liquid nitrogen and stored at -80°C unless used immediately. Cells were lysed in RIPA buffer (10 mM Tris pH 8,1 mM EDTA, 1% NP-40, 0.1% SDS, 140 mM NaCl, 0.1% Na-Deoxycholate and supplemented with protease inhibitor cocktail, 500 mM sodium fluoride, 100 mM phenylmethylsulfonyl fluoride, 1 M dithiothreitol, 25 U/µl Bezonase and 5 mg/ml Tosyl phenylalanyl chloromethyl ketone). Snap frozen cell pellets were thawed on ice and resuspended in lysis buffer. The mixture was incubated for 20 minutes on ice and insoluble material was removed by centrifugation for 30 minutes at 12500 rpm at 4°C. The supernatant was transferred to a new tube.

Protein concentrations of the samples were measured with a Bradford Assay. For this, standards of 5, 10,15,20,30 µg/ml of γ-globulin in Bradford protein assay reagent were prepared. The absorbance at 595 nm of standard samples was measured on a Spectrophotometer to generate a standard curve. Following this, 1 µl of lysate was added to 1 ml of Bradford assay reagent and the absorbance at 595 nm was determined. Protein

concentrations were calculated based on the standard curve. Samples were diluted to 5 µg/µl protein concentration using lysis buffer.

To separate proteins based on size, a 10% acrylamide gel was used. The running gel was prepared by mixing 1.5 M Tris-HCl pH 8.8, 10% SDS, 30% acrylamide and water. Polymerization was initiated by adding 10% APS and TEMED. Subsequently the stacking gel was prepared by mixing 0.5 M Tris-HCl pH 6.8, water and 30% acrylamide. Polymerization was initiated by adding 10% APS and TEMED. After the gel was fully polymerized, Lämmli buffer + β-mercaptoethanol was added to 50 µg of protein extracts and samples were boiled for 5 minutes at 95°C. The samples were allowed to cool down to room temperature, centrifuged and loaded onto the gel. The gel was run at 70 V until the samples reached the running gel, then the voltage was increased to 120 V and the gel was run until the bands nearly reached the bottom edge of the gel.

For the transfer of the proteins onto the nitrocellulose PTFE membrane, a transfer buffer consisting of 50 mM Tris[hydroxymethyl]aminomethane, 380 mM glycine, 10% methanol water was used. The filter paper and the nitrocellulose membrane were soaked in transfer buffer. The blotting chamber was assembled as follows: A filter paper soaked with transfer buffer was placed at the bottom of the chamber, then the nitrocellulose membrane was added. The gel was placed on top of the membrane and another filter paper was placed on top of the gel. Proteins were transferred to the membrane at 25 Volts,1 Ampere for 30 minutes in a BioRad Trans-Blot Turbo transfer system.

Following protein transfer the membrane was stained with Ponceau S solution while shaking for 10 minutes. A picture was acquired after the staining and the membrane was washed with water until the staining disappeared.

TBS buffer was prepared by dissolving 1.5 M NaCl in 0.5 M Tris-HCl and the pH was adjusted to 7.4. Subsequently TBS-T buffer was prepared by adding Tween20 (Sigma-Aldrich, Missouri USA) to the TBS buffer to reach a final concentration of 0.1% Tween20. The membranes were incubated for blocking in 5% low fat milk in TBS-T for 1 hour. Subsequently the membranes were incubated with the primary antibodies in 5% low fat milk overnight with shaking at 4°C as follows: antin-DDX6 (Novus Biologicals, Colorado USA, NB200-192, rabbit) at a dilution of 1:5000, anti-β-actin (Cell Signaling technology, Massachusetts USA, 8H10D10, mouse) at a dilution of 1:5000 and anti-HSC-70 (Santa Cruz Biotechnologies, Dallas USA, B2117, mouse)

at a dilution of 1:10000. on the next day, the membranes were washed twice with TBS-T for 5 minutes each. Following the washing steps, the membranes were incubated with the secondary antibodies (goat anti-rabbit: Cell signaling technology Massachusetts, USA; 7074P2; goat anti-mouse: Thermofisher Scientifc Massachusetts, USA; 31439) at a concentration of 1:10000 in 5% low fat milk in TBS-T for 1 hour at RT. After that, the membranes were washed twice for 5 minutes with TBS-T.

For imaging the Western blot, Amersham ECL prime luminol enhancer solution (Merck, Darmstadt Germany) was mixed with Amersham ECL prime peroxide solution (Merck, Darmstadt Germany) at a ratio of 1:1. The solution was added to the membrane, the membrane was placed in a transparent foil and imaged in a Vilber Fusion FX device. The images of the blot were acquired by using the standard settings of the program.

Antibody	Company and catalog number
Primary Rabbit anti DDX6	Novus Biologicals (Colorado, USA); NB200-192
Primary Mouse anti HSC70	Santa Cruz Biotechnologies (Dallas, USA); B2117
Primary Mouse anti β-actin	Cell signaling technology (Massachusetts, USA); 8H10D10
Secondary anti Rabbit HRP-linked	Cell signaling technology (Massachusetts, USA); 7074P2
Secondary anti Mouse HRP-linked	Thermofisher Scientifc (Massachusetts, USA); 31439

Table 4: Antibodies used in Western Blots

2.8) Immunofluorescence

Roughly, 500,000 to 1,000,000 cells were spotted onto glass slides by centrifugation at 700 rpm for 3 minutes using a Cytospin2 cytocentrifuge. Following this the cells were left to air dry in the dark for 30 minutes. Then the cells were fixed with 4.5% ROTI® Histofix in PBS for 10 minutes in the dark. Following the fixation two immediate washing steps with water were performed. Afterwards the cells were washed three times for 5 minutes with PBS. The cells were then permeabilized in 0.2% TritonX100 in PBS for 10 minutes at room temperature in the dark. Subsequently, slides were blocked in sterile filtered 2% BSA/ 0.2% TritonX100 in PBS for 1 hour in the dark. After the blocking the primary rabbit anti DDX6 Antibody (Novus Biologicals (Colorado, USA, NB200-192) at a dilution of either 1:300 or 1:400 in 2% BSA / 0.2% TritonX100 in PBS or the primary Rabbit anti EDC4 antibody (Abcam, Cambrdige UK, ab72408) at a dilution of 1:20 in 2% BSA / 0.2% TritonX100 in PBS was added and samples

were incubated overnight in a dark wet chamber at 4°C. On the next day, samples were washed three times in PBS for 5 minutes and then incubated for 1 hour in a dark wet chamber with anti-rabbit secondary antibody conjugated to Alexa Fluor 647 at a concentration of 1:2000 and 5 mg/ml DAPI at a dilution of 1:1000 in 2% BSA/0.2% TritonX100 in PBS. Then, slides were washed three times with PBS for 5 minutes each and samples were mounted in Entellan (Merck, Darmstadt Germany), covered with a glass slide 0.14 mm in diameter and air-dried.

Antibody	Company and Catalog Number
Primary Rabbit anti DDX6	Novus Biologicals NB200-192
Primary Rabbit anti EDC4	Abcam, ab72408
Secondary anti Rabbit Alexa Fluor 647	Invitrogen A21244

Table 5: Antibodies used in the Immunofluorescence

Immunofluorescence images were acquired using a Zeiss LSM-880 Airyscan confocal microscope. All images were obtained using a 63x magnification lens with oil as immersion media unless stated otherwise. Laser conditions were kept constant for all the images.

2.9) Image analysis

For the analysis of immunofluorescence imaging the Fiji package of ImageJ was used. To measure the average fluorescence intensity of DDX6 or EDC4 the colored multi-channel tiff file of each image was split into separate color channels thereby converting it into an 8-bit greyscale. Following this the red or green channel (for DDX6 or EDC4, respectively) was selected. Using the freehand selection tool of ImageJ the DDX6/EDC4 signal was highlighted by drawing a circle around the signal. Then the signal intensity was measured by using the measure function of ImageJ. The mean fluorescence intensity of all images was used to calculate the average signal intensity of each cell line.

To analyze the average amount of P-bodies per cell the colored multi-channel tiff file was split into its separate color channels thereby converting it into an 8-bit greyscale. The channel specific for DDX6 or EDC4 was selected and a threshold was set for each image individually to ensure that only P-body signals were visible. Then the analyze particle function of ImageJ was used to count the exact amounts of P-bodies in each image. Next, the total amount of cells was counted per image by using the DAPI channel, setting a threshold to highlight the nuclei and then using the analyze particle functions but adjusted to count nuclei based on the size. The total overall amount of P-bodies per image and the total amount of nuclei in each image was then used to calculate the average amount of P-bodies per cell for every image.

2.10) Statistics

Statistical analysis was performed using Microsoft Excel and Graphpad Prism 6. Mean fluorescence of the immunofluorescence images was measured using the ImageJ software. Experiments were performed in triplicates and repeated at least two times. The unpaired Student's t-test was used for p-value determination. Results were considered significant when $p < 0.05$ (*$p < 0.05$, **$p < 0.01$, ***$p < 0.001$, ****$p < 0.0001$).

3) Results

3.1) DDX6 is a genetic dependency in murine AML

Prior to this work, genome wide CRISPR/Cas9 dropout screens were performed (data not shown) to identify leukemia-specific genetic dependencies. In this setup, a Cas9-expressing clone of the immortalized murine AML cell line CNC (*CEBPA* N-term mutant / C-term mutant, used as a model for AML with biallelic CEBPA mutations) was compared to Cas9-expressing murine HPC-7 cells as a representative of healthy, untransformed hematopoietic progenitor cells. The analysis of these datasets indicated that components of P-bodies such as DDX6, AGO2 DCP1A, DCP2, EDC4 and CAPRIN1 could represent AML-specific genetic dependencies. With the aim of validating our findings, we performed a competition-based proliferation assay (Fig. 4a) in Cas9-expressing HPC-7 and CNC cells by using two sgRNAs (single guide RNAs) targeting P-body-associated genes. As shown in Figure 4b, CRISPR/Cas9-induced mutational disruption of *Ddx6, Ago2, Dcp1a, Dcp2, Edc4* and *Caprin1* did not affect the proliferative capacity of HPC-7 cells, but caused a strong fitness disadvantage in CNC cells, confirming what the results of the genome wide loss-of-function screens. We decided to focus our attention on DDX6, since this gene showed the highest depletion score among P-body components when the two CRISPR/Cas9 screen datasets were intersected (Fig. 4c). In addition, Ddx6 knockout had the most dramatic effect on CNC cell proliferation (Fig. 4b). Protein analysis via western blot showed that DDX6 protein levels were similar between the two cell lines (Fig. 4d), we found that *DDX6* mRNA was expressed at significantly higher levels in murine AML cells compared to HPC-7 cells (Fig. 4e). This indicates that *DDX6* mRNA expression is upregulated either during or following malignant transformation in murine cells whereas a mechanism of post-transcriptional regulation might prevent an increase in DDX6 protein levels.

a

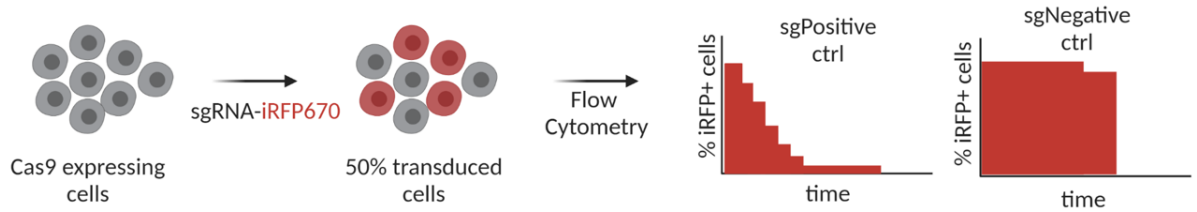

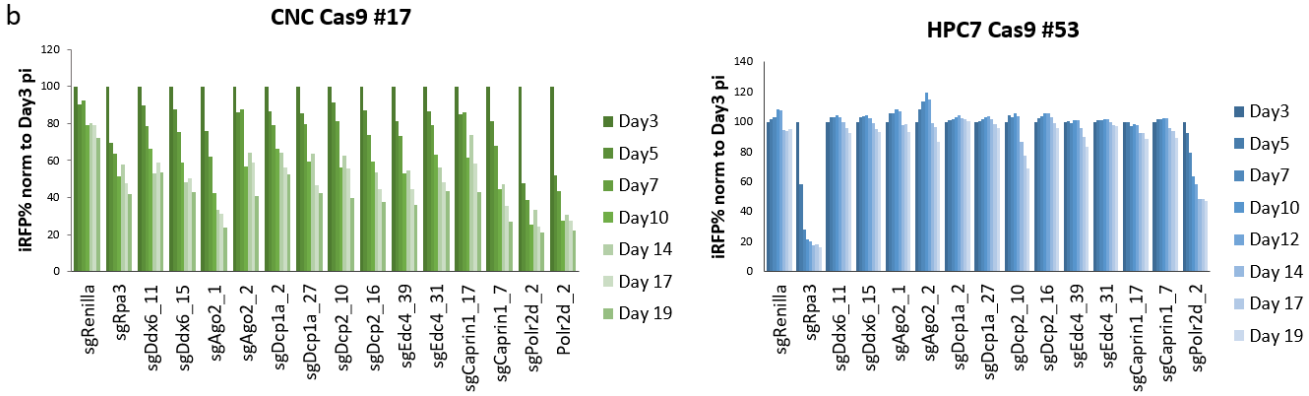
b
CNC Cas9 #17
iRFP% norm to Day3 pi
sgRenilla
sgRpa3
sgDdx6_11
sgDdx6_15
sgAgo2_1
sgAgo2_2
sgDcp1a_2
sgDcp1a_27
sgDcp2_10
sgDcp2_16
sgEdc4_39
sgEdc4_31
sgCaprin1_17
sgCaprin1_7
sgPolr2d_2
Polr2d_2
Day3
Day5
Day7
Day10
Day 14
Day 17
Day 19
HPC7 Cas9 #53
iRFP% norm to Day3 pi
sgRenilla
sgRpa3
sgDdx6_11
sgDdx6_15
sgAgo2_1
sgAgo2_2
sgDcp1a_2
sgDcp1a_27
sgDcp2_10
sgDcp2_16
sgEdc4_39
sgEdc4_31
sgCaprin1_17
sgCaprin1_7
sgPolr2d_2
Day3
Day5
Day7
Day10
Day12
Day 14
Day 17
Day 19

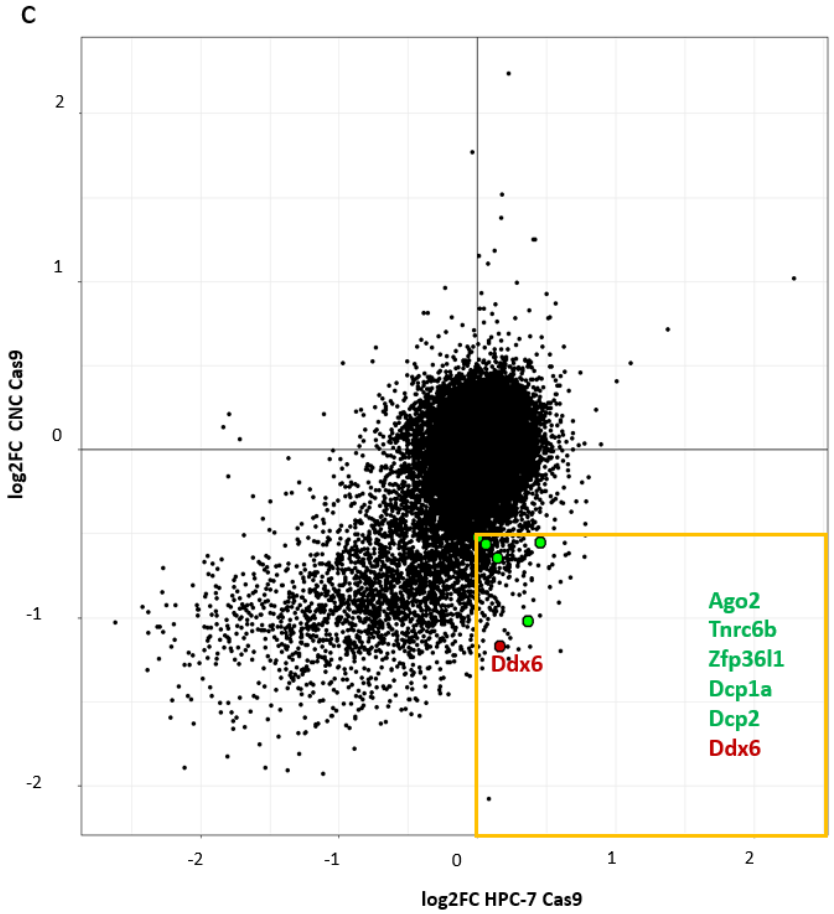
C
log2FC CNC Cas9
log2FC HPC-7 Cas9
Ago2
Tnrc6b
Zfp36l1
Dcp1a
Dcp2
Ddx6
Ddx6

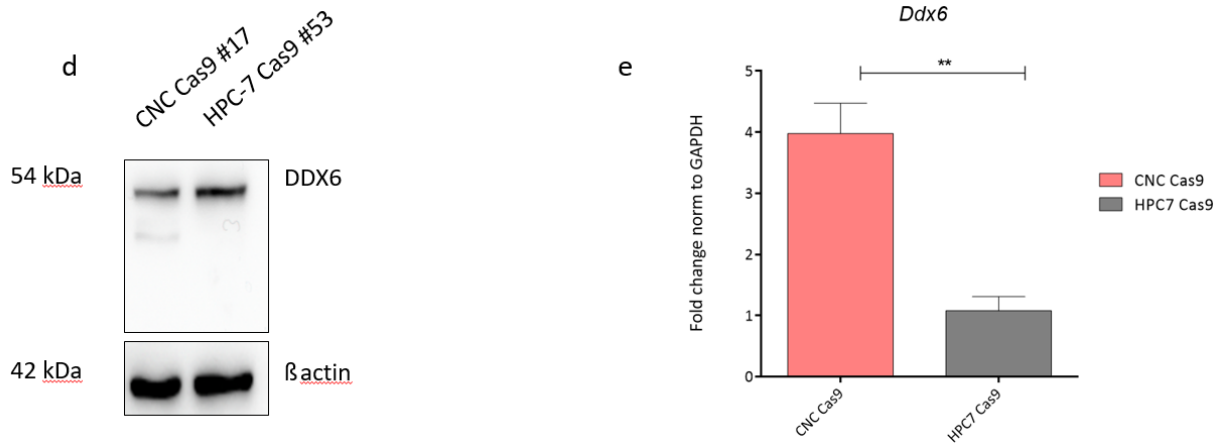

Figure 4: **Analysis of P-body genes and DDX6 in the murine HSPC line HPC-7 and the murine AML cell line CNC**. a) Schematic overview of the competition-based proliferation assay. b) Competition-based proliferation assay utilizing CRISPR/Cas9-mediated knockout in murine AML cell lines using 2 guide RNAs each targeting genes associated with P-body function. sgRNAs targeting Renilla and Rpa3 served as controls. Percentages of iRFP-positive cells were normalized to day 3 post transduction. Measurements were performed every 2-3 days. Bars indicate the mean of 2 biological replicates. c) Intersection of 2 genome wide CRISPR Cas9 dropout screens in the murine HSPC line HPC-7 and in the murine AML cell line CNC. DDX6 showed the highest depletion score among all the analyzed genes. d) Western blot analysis of murine HSPCs and murine AML cells using the indicated antibodies e) DDX6 RNA expression analysis using RT-qPCR. Bars indicate fold change of gene expression normalized to GAPDH using 3 biological replicates in triplicates.

3.2) DDX6 is a leukemia genetic dependency in human AML cells.

Since DDX6 was identified as a leukemia-specific genetic dependency in our mouse model for AML with biallelic *CEBPA* mutations, we next investigated the role of DDX6 in human AML. We took advantage of the DepMap portal (https://depmap.org/portal/), where publicly available genome-wide CRISPR/Cas9 screening datasets are deposited. Among them, 26 distinct datasets represent AML cell. In addition, we investigated the genome-scale CRISPR/Cas9 loss of function screening dataset generated by Wang and colleagues (Wang et al. 2017), where 14 different AML cell lines were analyzed. DDX6 had a clear negative essentiality score in both datasets, indicating that DDX6 is needed for the proliferation and survival of AML cells and is indeed a genetic dependency in human AML cells (Fig. 5a). In comparison to this, the PLA2G16 gene, which encodes the adipocyte phospholipase A2 did not represent a dependency in human AML cell lines, whereas c-Myc showed a highly negative score in the Depmap data (Fig 5a). To confirm our findings, we performed a competition-based proliferation assay using four sgRNAs targeting DDX6 in Cas9-expressing human AML cell lines MOLM13,

THP-1, HL60 and MV411. As displayed in Fig 5b-e the knockout of *DDX6* had a strong negative effect on the proliferation capabilities of human AML cells. To further validate DDX6 as an important player in the maintenance of leukemia cells survival, we also downregulated *DDX6* expression by short hairpin RNAs (shRNAs). Both shRNAs targeting DDX6 caused a time-dependent depletion of shRNA-expressing cells. Expression of positive control shRNAs targeting RPL17, which is an essential gene of the 60S ribosomal subunit, led to a time-dependent depletion of shRNA containing cells, whereas the negative control shRenilla showed no change in iRFP670 signal (Fig. 5f-i). This indicates that also the knockdown of DDX6 caused a reduction in the proliferative capacity of human AML cells and confirms the results of the competition-based proliferation assay using CRISPR/Cas9 mediated gene knockout (Fig.5b-e). Taken together, these data show that DDX6 is a genetic dependency in human AML cells.

a

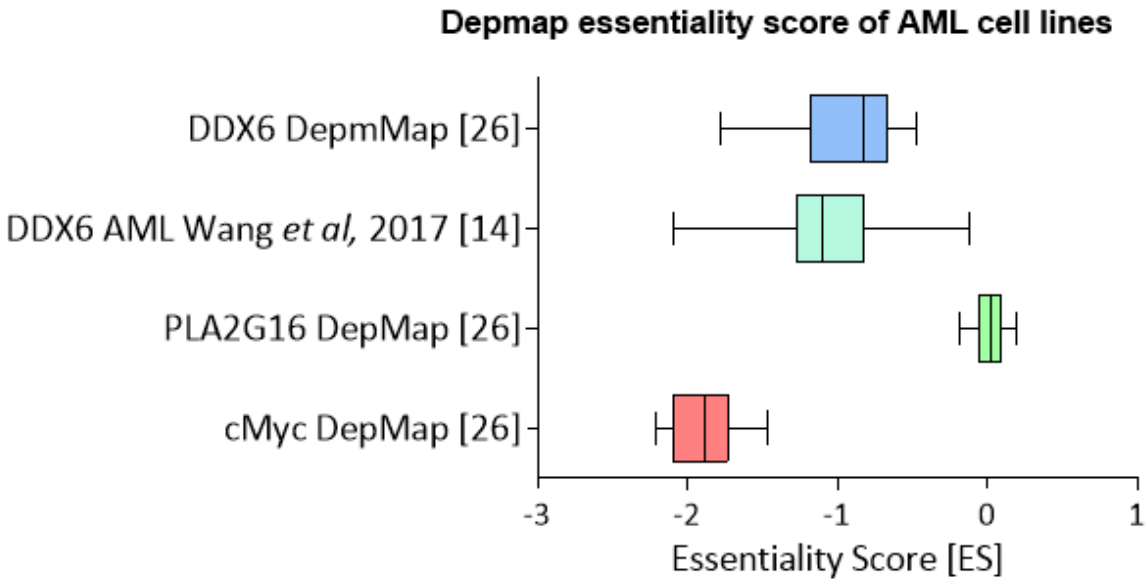

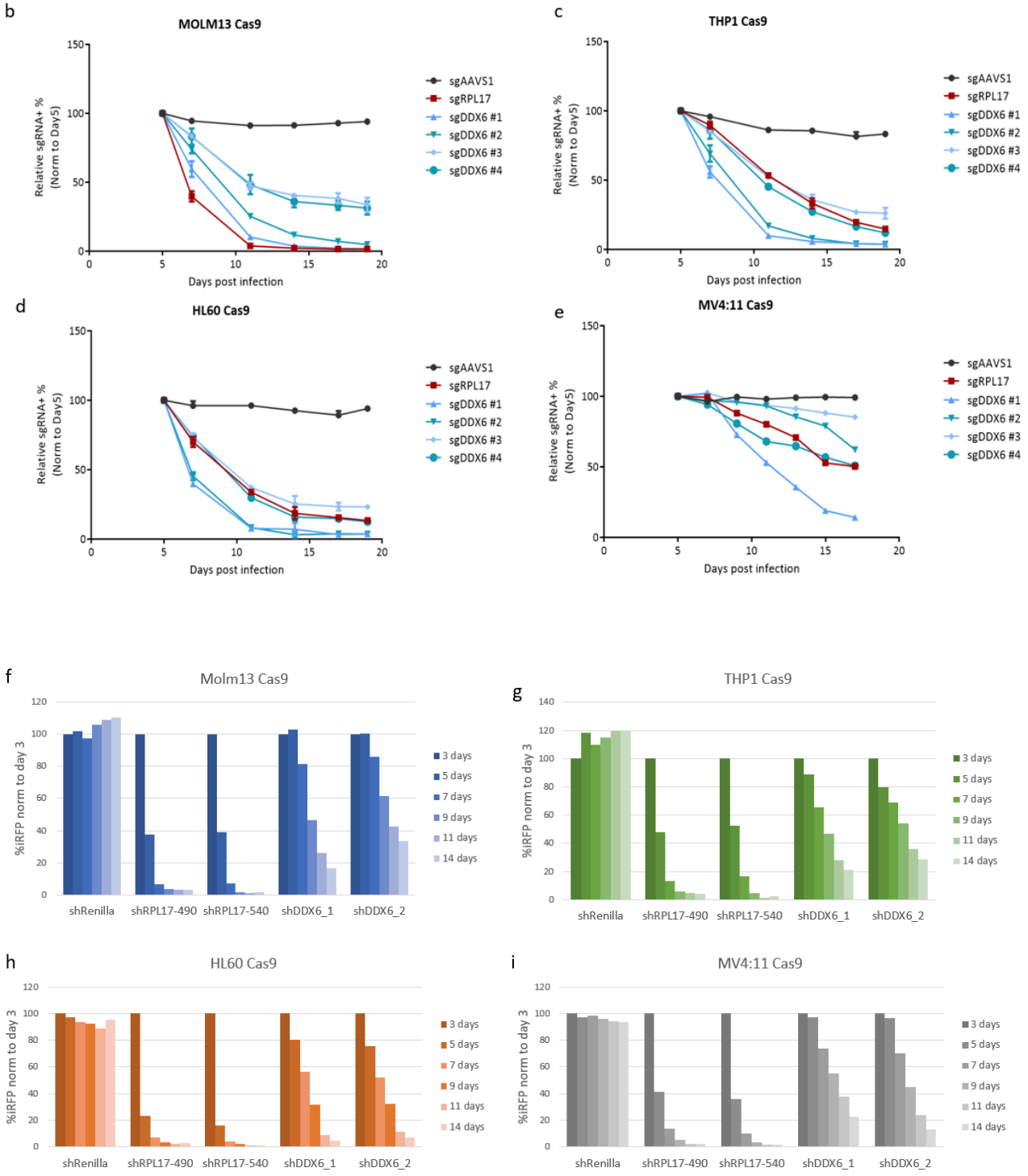

Figure 5: Effect of DDX6 knockout and knockdown on human AML cell proliferation. a) Essentiality score of DDX6 in the Depmap dataset (https://depmap.org/portal/) of 26 AML cell lines and 14 AML cell lines from the Wang et al study (Wang et al. 2017). Essentiality score of c-Myc, a known genetic dependency in human AML cells and PLA2G16 a gene known to show no dependency in AML from the Depmap dataset (https://depmap.org/portal/) of 26 AML cell lines. b-e) Competition-based proliferation assay utilizing CRISPR/Cas9-mediated knockout in human AML cell lines using 4 guide RNAs targeting DDX6.

Percentages of iRFP670 positive cells were normalized to day 3 post transduction. Measurements were performed every 2-3 days. Bars indicate the mean of 2 biological replicates f-i) Competition-based proliferation assay using two shRNAs to target DDX6 in human AML cell lines. Percentages of iRFP670 positive cells were normalized to day 3 post transduction of the respective shRNAs. Measurements were performed every 2-3 days. Bars indicate the mean of 2 biological replicates.

3.3) DDX6 expression is upregulated in human AML

To further explore DDX6's role in human AML, we assessed the expression pattern of *DDX6* in patient samples and human AML cell lines. Investigation of the Gene Expression Profiling Interactive Analysis (GePIA2) database showed that across all cancer types, the mRNA expression levels of *DDX6* were highest in AML patient samples (Fig. 6a). Furthermore, *DDX6* mRNA was expressed at higher levels in AML patient samples than in healthy donors, in line with our findings in murine AML cells (Fig. 6b). To validate these findings, we measured *DDX6* mRNA expression using RT-qPCR in the human AML cells THP1, MV4:11, HL60 and MOLM13. Human placenta CD34+ cells served as controls. We observed that *DDX6* expression was significantly higher in all human AML cells than in the placenta-derived CD34+ cells, with the exception of THP1 (Fig. 6c). Next, we measured DDX6 protein levels in the same human AML cell lines, the placenta derived CD34+ cells, HEPG2 cells (liver hepatocellular carcinoma) and the HEK-derived 293T cell line. We observed that DDX6 protein levels were similar between human AML cell lines and CD34+ placenta cells. HEPG2 cells showed the lowest DDX6 protein levels among all samples (Fig. 6d). These findings not only confirm the data from AML patient samples but also corroborate our results obtained in murine cells, as they confirm that *DDX6* mRNA is higher expressed in AML cells than in healthy, untransformed cells. Taken together, these findings indicate that DDX6 expression is dysregulated in leukemia.

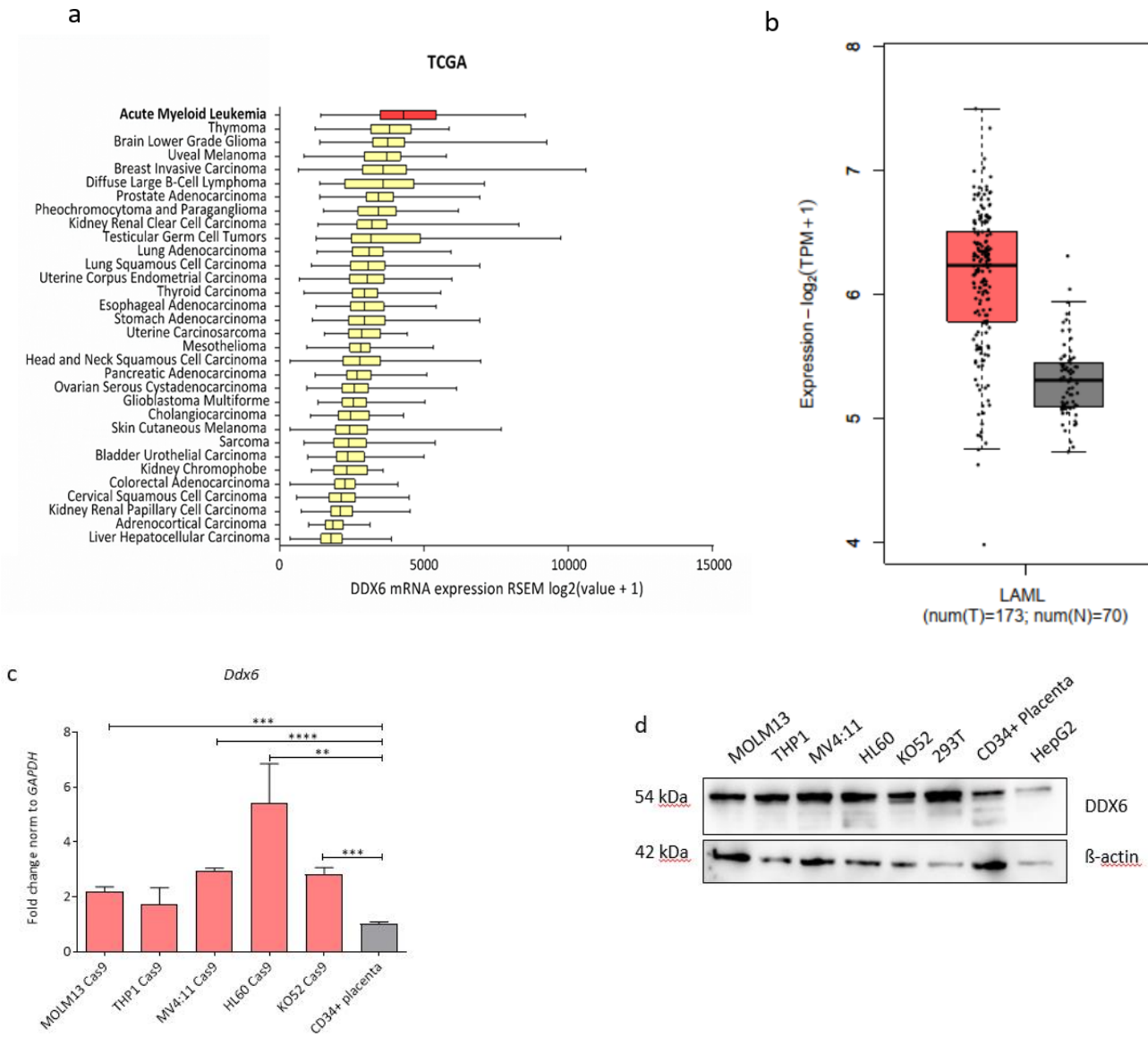

Figure 6: Analysis of DDX6 mRNA and protein expression. a) Analysis of publicly available patient samples from different cancer types for DDX6 mRNA expression using the web tool GEPIA (http://gepia.cancer-pku.cn/index.html). b) GEPIA2 analysis of DDX6 mRNA levels between patients with AML and healthy donor samples (http://gepia2.cancer-pku.cn/#index. c) Gene expression analysis of DDX6 in different human AML cell lines and CD34+ placenta cells using RT-qPCR. Bars indicate fold change normalized to GAPDH using 3 biological replicates each in triplicates. P-values were determined using unpaired student's t-test (*p < 0.05, **p < 0.01, ***p < 0.001, ****p < 0.0001). d) DDX6 protein analysis of different human AML cells, CD34+ placenta cells, the hepatocellular carcinoma derived cell line HEPG2 and the HEK-derived cell line 293T using western blotting.

3.4) Immunofluorescence imaging of DDX6 reveals its accumulation in distinct cytoplasmic foci in human and murine AML cells

As it has been reported that DDX6 localized to distinct cytoplasmic foci termed P-bodies in HeLa cells (Andrei et al. 2005) we wanted to investigate if DDX6 also localizes to P-bodies in human and murine AML cells. To this end we utilized immunofluorescence imaging using an anti-DDX6 antibody. Upon quantification of the average DDX6 signal intensity in the human AML cell lines we found that MOLM13 and MV4:11 showed significantly higher average fluorescence intensities than THP1 and HL60 cells. We also quantified the average signal intensity in the murine cell lines and could not observe any significant difference in signal intensities between HPC-7and CNC lines (Fig. 7a). Furthermore, we observed that DDX6 indeed accumulated in distinct cytoplasmic foci in AML cell lines, confirming the findings obtained in other cell systems (Fig. 7b).

a

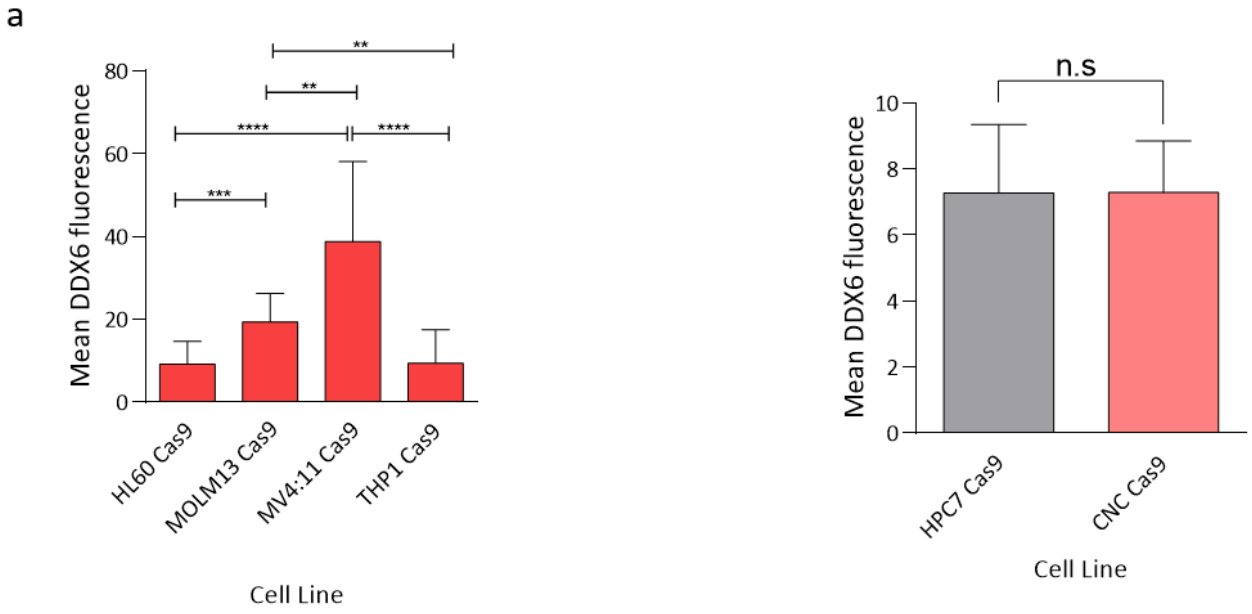

b

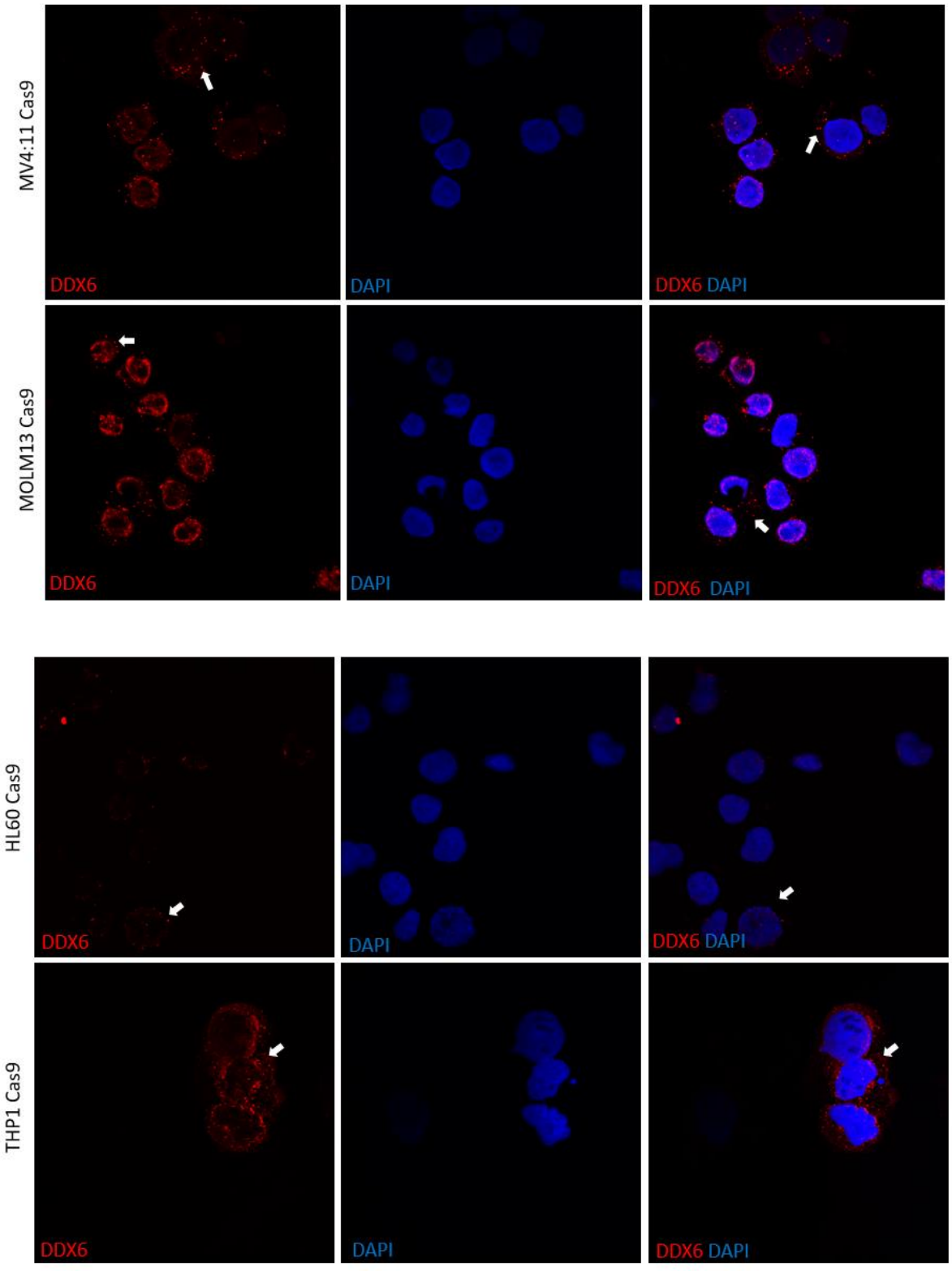
MV4:11 Cas9
DDX6
DAPI
DDX6 DAPI
MOLM13 Cas9
DDX6
DAPI
DDX6 DAPI
HL60 Cas9
DDX6
DAPI
DDX6 DAPI
THP1 Cas9
DDX6
DAPI
DDX6 DAPI

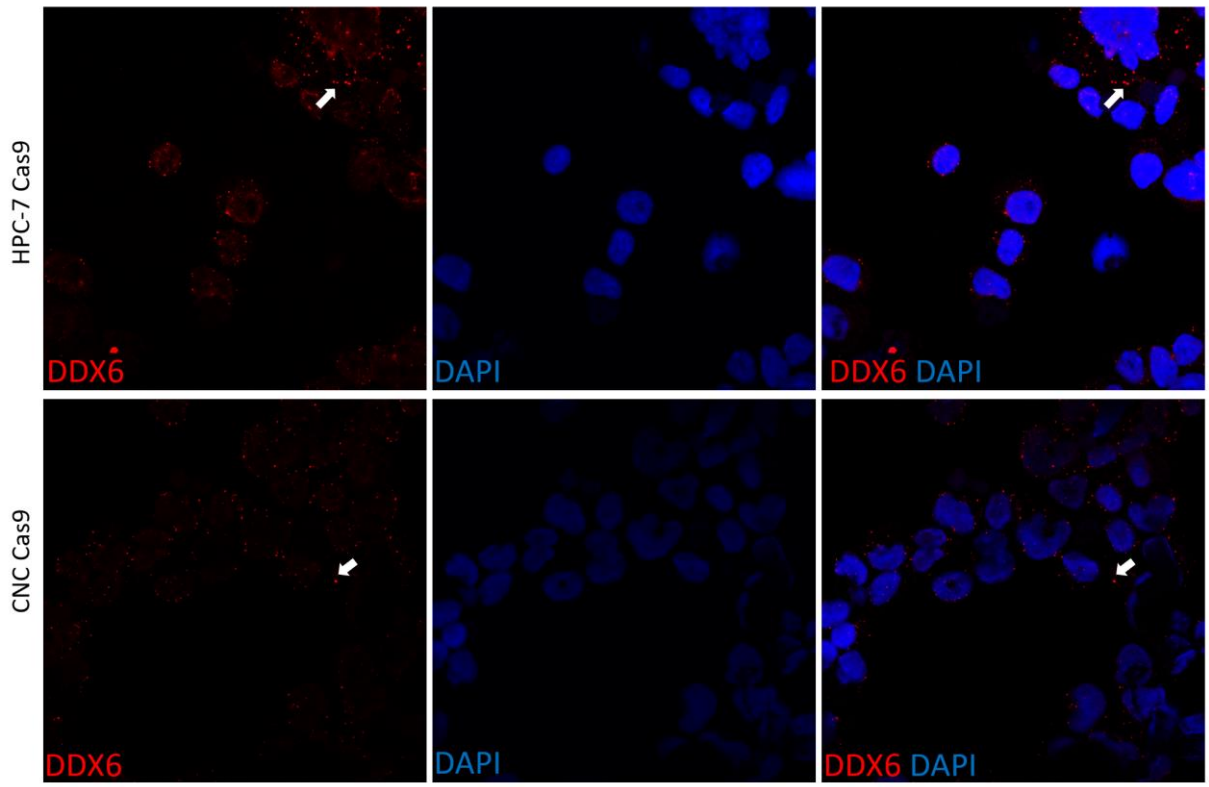

Figure 7: DDX6 image analysis of human and murine AML cells. a) Mean DDX6 fluorescence was measured using the measure function of Fiji ImageJ on the red channel for DDX6. Bars indicate the results of 12 images with at least 4 cells per image. b) Pictures of human AML cells stained with rabbit anti DDX6 primary antibody were obtained using a Zeiss LSM-880 Airyscan confocal microscope with a 63x magnification lens and using oil as immersion media. White arrows indicate cytoplasmic foci of DDX6 accumulation.

3.5) Staining with the P-body marker EDC4 reveals the presence of cytoplasmic P-bodies in human acute myeloid leukemia cells

The presence of P-bodies has been reported in many different cells (Hubstenberger et al. 2017). However, their presence has not yet been shown in human AML cell lines. To test if our cells display P-bodies we utilized immunofluorescence imaging with an anti-EDC4 antibody, which is a known P-body marker (Hubstenberger et al. 2017). First, we quantified the average EDC4 signal intensity and found that only MOLM13 cells displayed a significantly higher average EDC4 signal among all cell lines tested by us (Fig. 8a). Next, we also observed that all human AML cell lines displayed distinct cytoplasmic accumulation of EDC4 signal which in

fact are P-bodies (Fig. 8b). These findings prove that P-bodies are indeed also present in human AML cell lines.

a

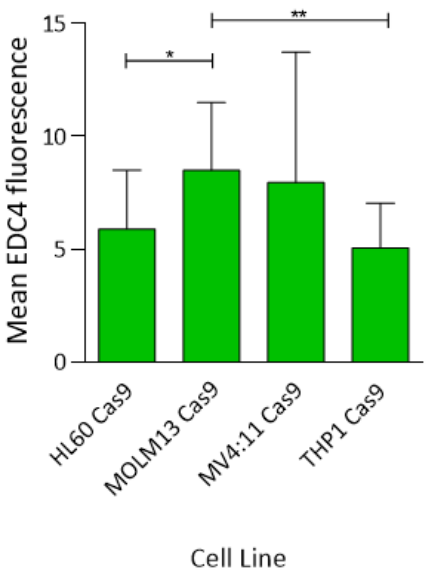

b

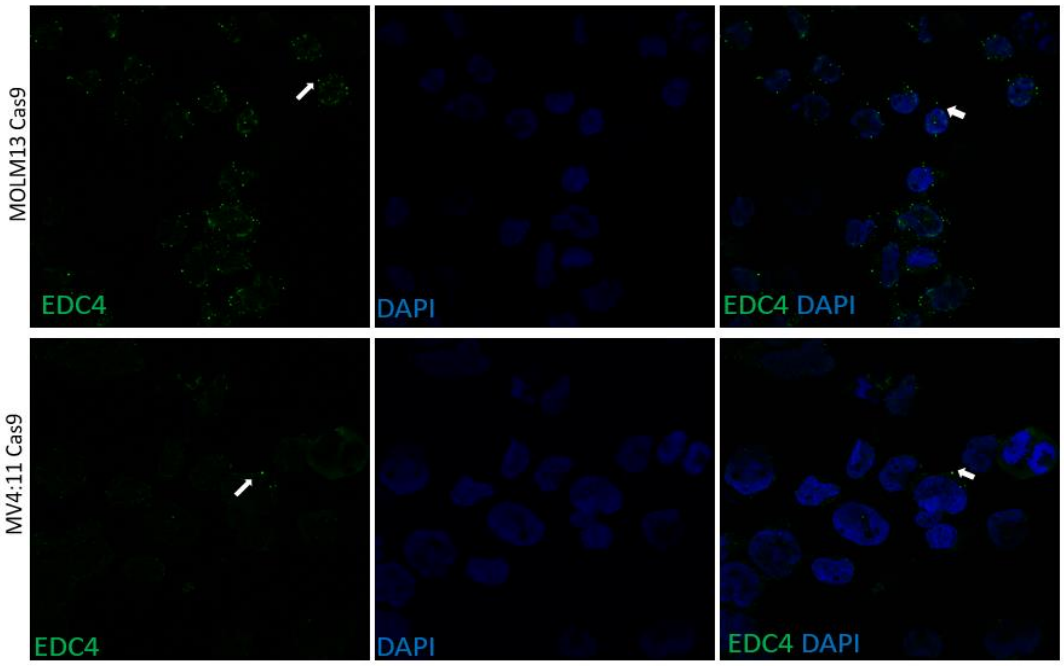

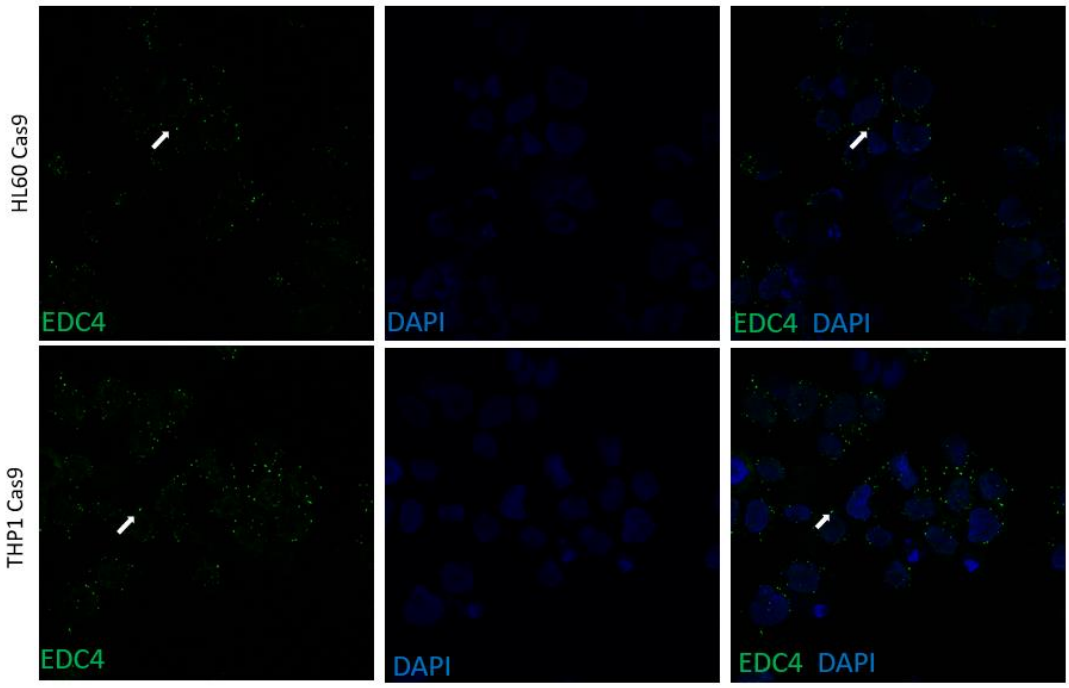

Figure 8: EDC4 imaging analysis of human and murine AML cells. a) Mean EDC4 fluorescence was measured using the measure function of Fiji ImageJ on the green channel for EDC4. Bars indicate show the results of 12 images with at least 4 cells per image. b) Pictures of human AML cells stained with rabbit anti EDC4 primary antibody were obtained using a Zeiss LSM-880 Airyscan confocal microscope with a 63x magnification lens and using oil as immersion media. White arrows indicate cytoplasmic foci of EDC4 accumulation.

3.6) Quantification of P-body numbers reveals DDX6 as a P-body marker in human AML cell lines

Since observe that DDX6 accumulated in distinct cytoplasmic foci, we wanted to know whether or not those structures are indeed P-bodies. To test this, we quantified the average amount of P-bodies per cell in our AML cell lines by combined analysis of DDX6 and the known P-body marker EDC4 (Hubstenberger et al. 2017). We utilized the analyze particle function of Fiji ImageJ. By setting a threshold that only allowed us to count the P-bodies based on EDC4 or DDX6 signals in our images and then quantifying the number of cells by using DAPI we were able to estimate the average number of P-bodies per cell. We found that THP-1 cells exhibited a significant difference in the number of P-bodies when DDX6 or EDC4 were used for quantitation. In all our other cell lines, the average amount of P-bodies per cell was similar (Fig.

9a). We also investigated the numbers of P-bodies in the murine AML cell lines. However, we were only able to do so using DDX6 because we discovered issues regarding the secondary antibody in our murine cells since. These cells are already PE positive and since the expression of our short hairpin RNAs is coupled to iRFP we could not use either Alexa 647 or PE. We did not observe any significant difference in the average amount of P-bodies between HPC-7 and CNC cell lines (Fig. 9b). Our findings suggest that in addition to EDC4, DDX6 also serves as a marker for P-bodies in human AML cell lines.

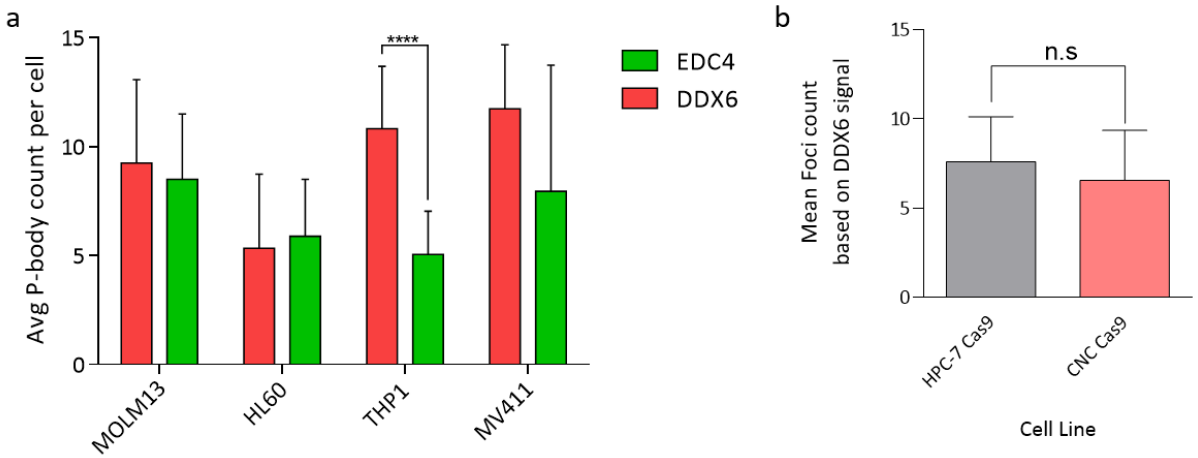

Figure 9: P-body quantification in human AML cell lines a&b) Average P-body count was obtained by setting a threshold to only visualize P-bodies as single pixels and subsequently using the analyze particles function of ImageJ to estimate overall P-body amount per image, counting the nuclei with DAPI and then calculating the average P-body amount per cell. Bars indicate the results of 12 images with at least 4 cells per image.

3.7) Doxycycline-inducible knockdown of DDX6 shows a time-dependent depletion of DDX6 protein levels.

As our previous experiment showed that both CRISPR/Cas9-mediated knockout and shRNA-induced knockdown of DDX6 led to a proliferative disadvantage in human AML cell lines (Fig. 5b-i) we wanted to gain a better understanding of the dynamic effects upon DDX6 loss. To study this we used a doxycycline-inducible shRNA mediated knockdown system targeting DDX6 by coupling the same short hairpin RNA sequences targeting the *DDX6* mRNA we used previously (Fig.5 f-i) to a doxycycline inducible expression system. In this system, shRNA expression is driven by a Tetracycline-inducible promoter Tet-On, (Zuber, McJunkin, et al. 2011). The doxycycline-dependent transcriptional activator protein (rtTA3) only binds to the

Tet operator sequence to induce expression of the shRNA in the presence of doxycycline (Zuber, Rappaport, et al. 2011). We used a lentiviral transduction system to stably integrate the constructs into the genome of the human AML cell lines MOLM13, THP-1, HL60 and MV4:11 that were previously engineered to express rtTA3 coupled to the ecotropic receptor (RIEP) for increased biological safety (Schambach et al. 2006). The initial induction efficiency 24 hours after doxycycline induction ranged from 30-45% in MOLM13 to over 90% in MV4:11. These cells were then used for our competition-based proliferation assays. In which, we observed a significant time-dependent decrease in iRFP670-positive shRNA-expressing cells upon doxycycline-induced knockdown of *DDX6* (Fig. 10 a-d) over time. This effect was similar to the effects we previously observed with the constitutive shRNA system (Fig. 5f-i).

To characterize the kinetics of the inducible *DDX6* knockdown we collected RNA samples before and 72 hours after doxycycline induction and analyzed *DDX6* mRNA expression via RT-qPCR. We found a significant depletion of DDX6 mRNA levels in MOLM13, HL60 and THP-1 72 hours post doxycycline induction with shDDX6_1 (Fig. 10e). In MV4:11 cells however, only shDDX6_2 significantly reduced *DDX6* mRNA levels whereas shDDX6_1 only induced a slight reduction of *DDX6* expression. To further validate the findings of the mRNA analysis we collected protein samples at various time points before and after doxycycline induction and analyzed DDX6 expression by western blotting. We found a time-dependent depletion of DDX6 protein levels in MOLM13 cells expressing shDDX6_1 and shDDX6_3 with almost no protein signal left after 72 hours of doxycycline treatment. shDDX6_2 only caused a slight depletion of DDX6 levels in MOLM13 cells (Fig. 10f). In HL60 cells, only a mild depletion of DDX6 protein levels could be observed upon expression of shDDX6_2, whereas shDDX6_1 and shDDX6_3 did not lead to a reduction of DDX6 protein levels 72 hours after doxycycline treatment (Fig. 10f). DDX6 protein levels were reduced in THP-1 transduced with shDDX6_3. However, shDDX6_1 and shDDX6_2 did not cause any visible reduction of DDX6 signal THP-1 (Fig. 10f). Finally, in MV4:11 cells shDDX6_1 and shDDX6_3 caused a time-dependent depletion of DDX6 protein levels with the strongest depletion after 72 hours, while shDDX6_2 only showed a slight reduction in DDX6 protein levels (Fig. 10f). Altogether our mRNA expression and protein analyses suggest that 72 hours post induction could represent an optimal time point to study the effects of DDX6 on the dynamics of RNA metabolism and post-transcriptional regulation of gene expression.

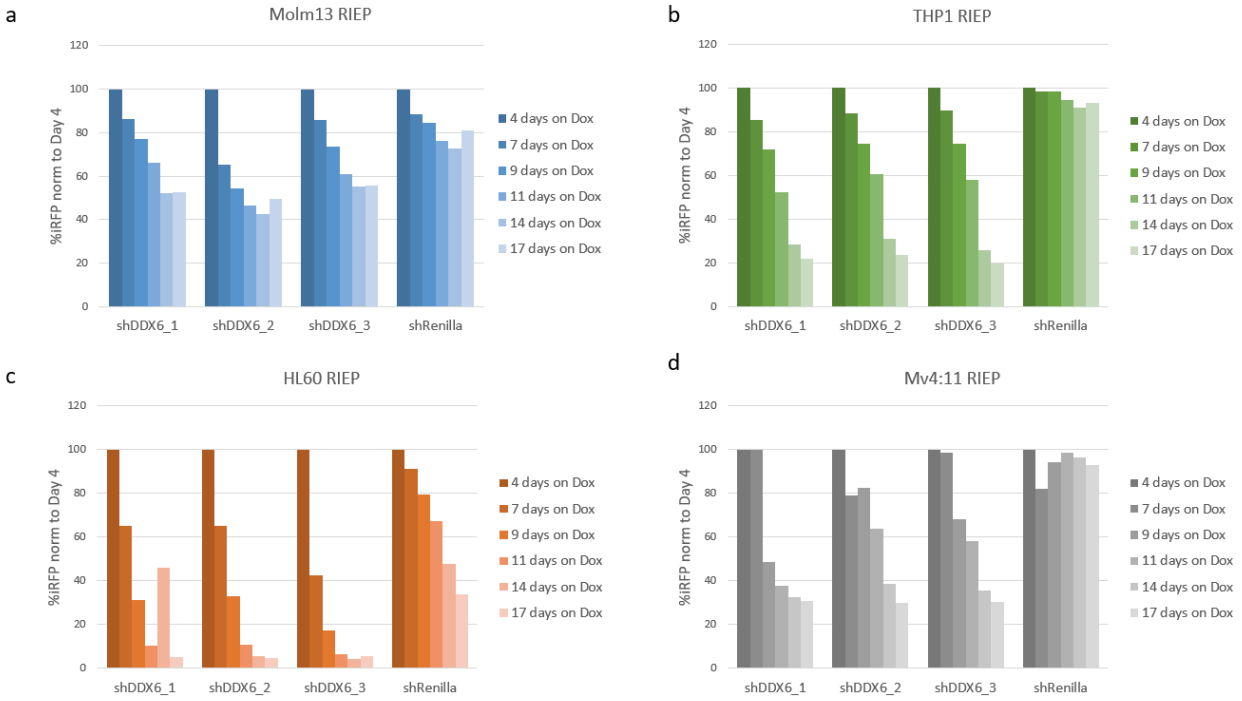
a
Molm13 RIEP
b
THP1 RIEP
c
HL60 RIEP
d
Mv4:11 RIEP
%iRFP norm to Day 4
120
100
80
60
40
20
0
shDDX6_1
shDDX6_2
shDDX6_3
shRenilla
4 days on Dox
7 days on Dox
9 days on Dox
11 days on Dox
14 days on Dox
17 days on Dox

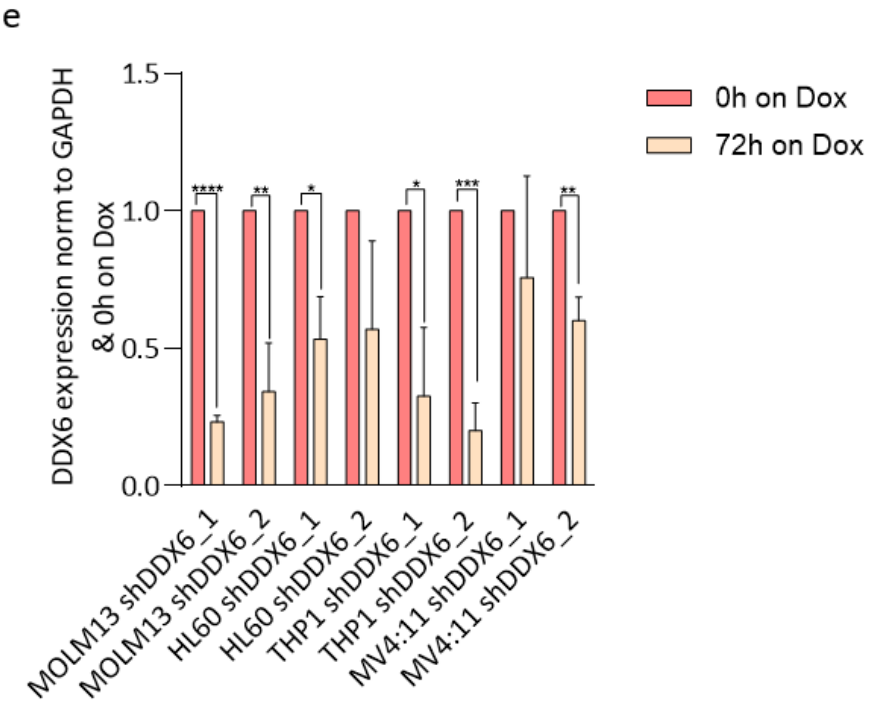
e
DDX6 expression norm to GAPDH & 0h on Dox
1.5
1.0
0.5
0.0
0h on Dox
72h on Dox
****
**
*
*
***
**
MOLM13 shDDX6_1
MOLM13 shDDX6_2
HL60 shDDX6_1
HL60 shDDX6_2
THP1 shDDX6_1
THP1 shDDX6_2
MV4:11 shDDX6_1
MV4:11 shDDX6_2

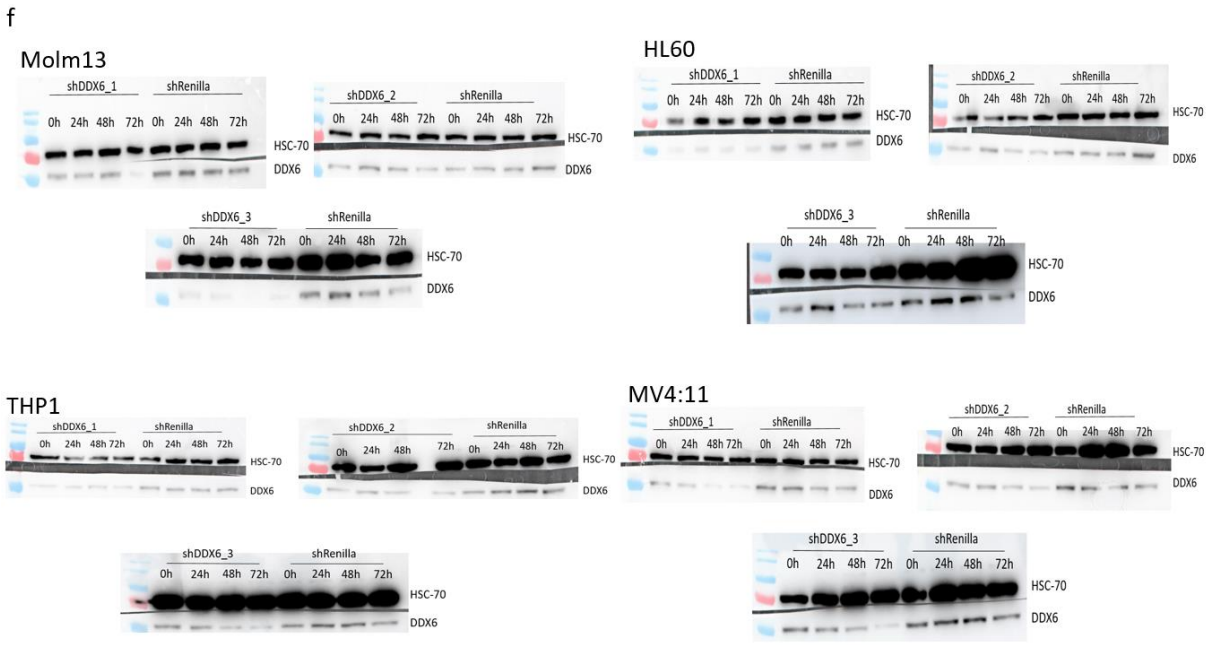

Figure 10: Doxycycline inducible DDX6 knockdown. a-d) Human AML cell lines with a Doxycycline inducible DDX6 knockdown were generated via lentiviral transduction. Following induction, percentages of iRFP-positive cells was measured every 2-3 days. Counts were normalized to day 3 post induction of the respective shRNAs. Bars indicate the mean of two biological replicates. e) Gene expression analysis in human AML cell lines transduced with our Doxycycline inducible shRNAs using RT-qPCR. Bars indicate the fold change normalized to GAPDH and to 0 hours on Doxycycline treatment using three biological replicates in technical triplicates. P-values were determined using unpaired student's t-test (*p < 0.05, **p < 0.01, ***p < 0.001, ****p < 0.0001). f) Western blot analysis of depletion kinetics after DDX6 knockdown.

3.8) DDX6 is essential for P-body maintenance in human AML

It has been reported that DDX6 is essential for eukaryotic P-body formation and maintenance and its role has been largely studied in the context of stem cells, progenitor cells as well as cancer cells (Wang et al. 2015) in both mice and humans. However, its role in AML remains unexplored. To test if DDX6 is a key player in the maintenance of P-body homeostasis in AML we made use of our doxycycline-inducible knockdown system to investigate the effect of DDX6 loss on P-bodies using confocal microscopy in human AML cell lines. In line with the results obtained by western blotting and qPCR, we observed a decrease in the DDX6 signal 72 hours after Doxycycline induction (Fig. 11a). Next, we tested if DDX6 loss resulted in a decrease in the absolute numbers of P-bodies. 72 hours after *DDX6* knockdown we detected a significant depletion of P-body counts in all the human AML cell lines when the signals from the DDX6- and EDC4-stainings were used for P-body quantification. This indicates that DDX6 expression is required for the maintenance of P-body integrity (Fig 11b, c). Collectively our data

demonstrate that DDX6 is essential for P-bodies assembly and its loss impairs P-bodies formation in AML.

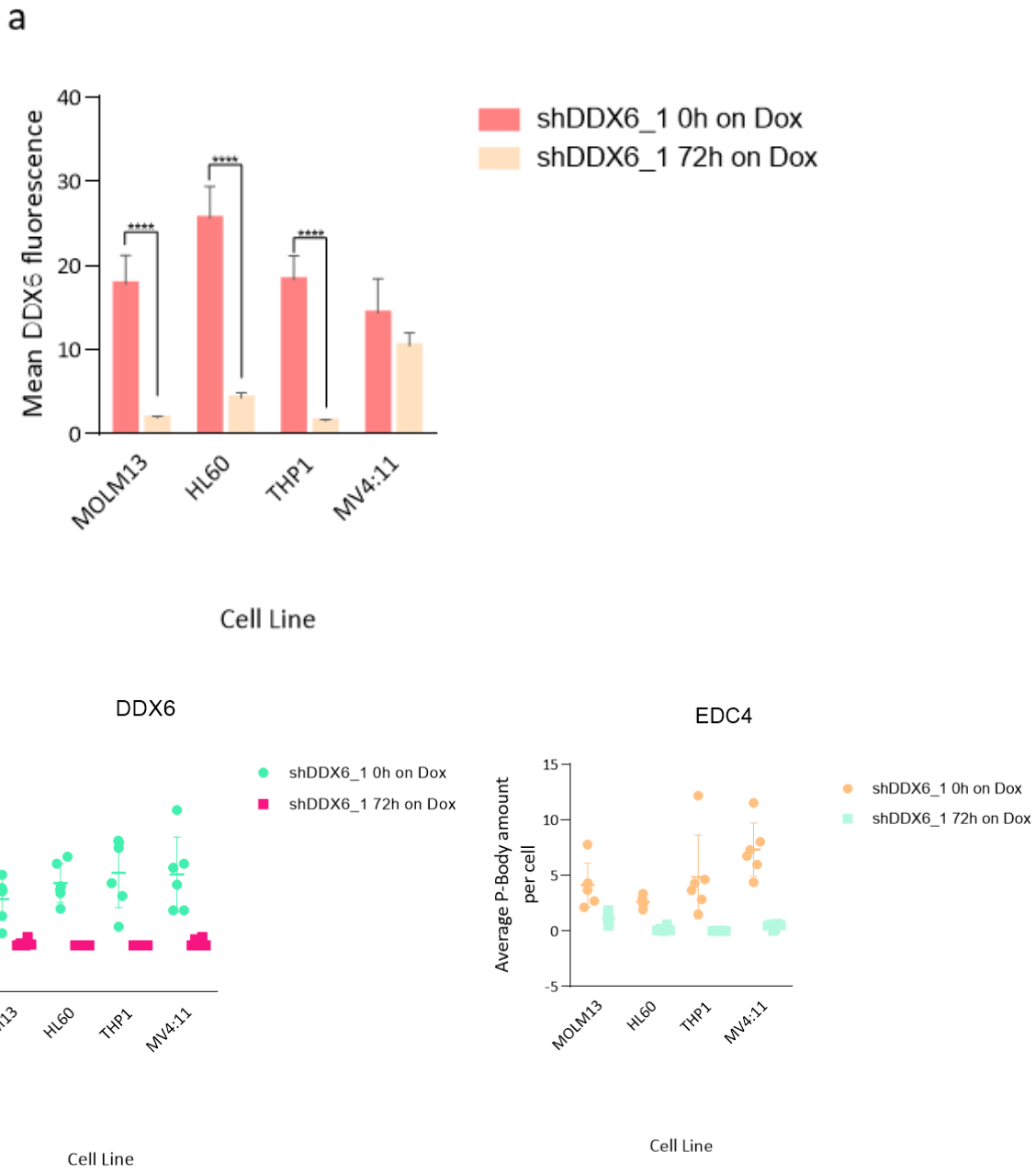

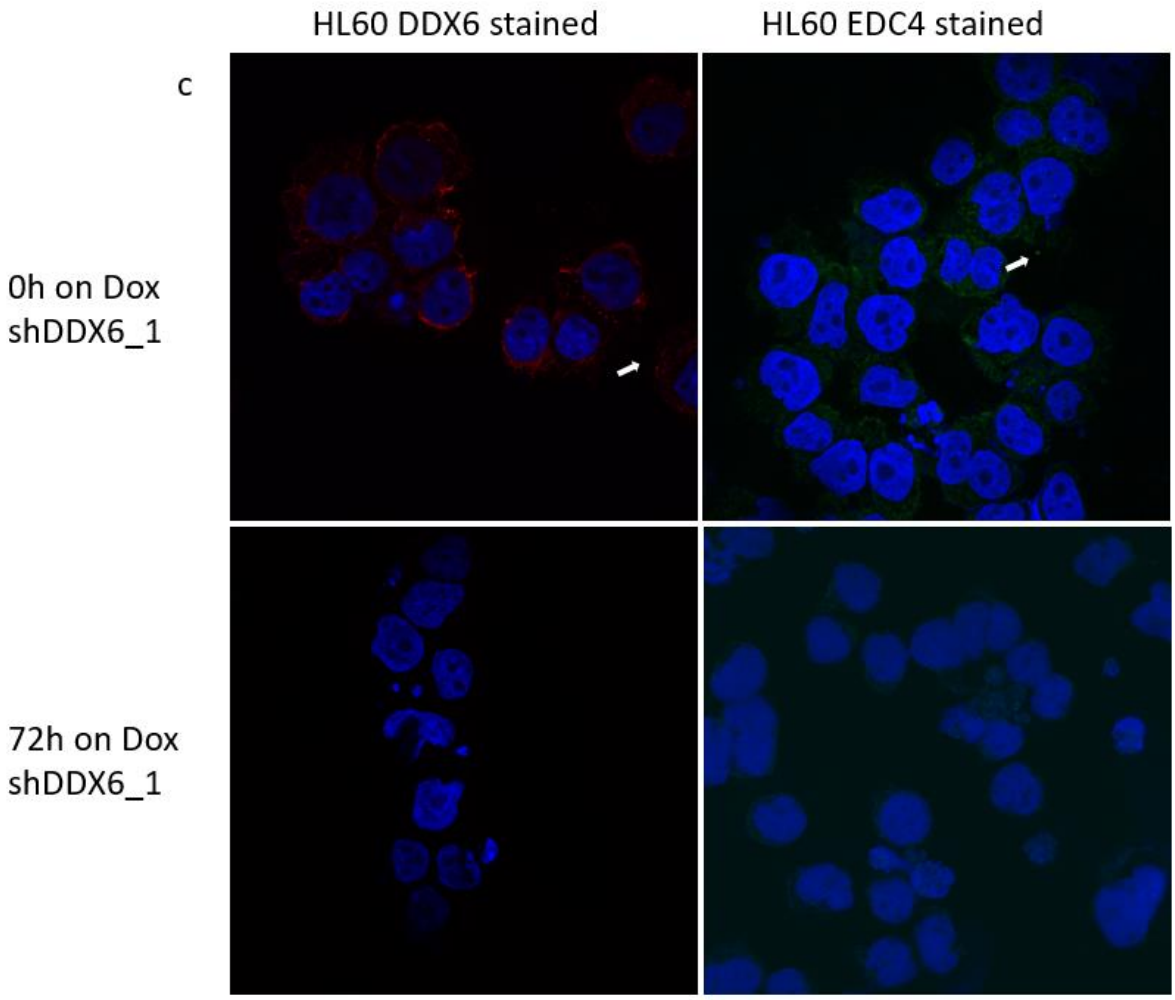

Figure 11: DDX6 is essential for P-body maintenance in human AML cell lines. a) Mean DDX6 fluorescence was measured prior and 72 hours post knockdown induction using the "measure" function of Fiji ImageJ on the red channel for DDX6. Bars show the results of 6 images with at least 4 cells per image. b) Average P-body counts were obtained by using the "analyze particles" function of ImageJ prior to and 72 hours after knockdown induction. To estimate overall P-body amounts per image, counting the nuclei and subsequently calculating the average P-body amount per cell. Bars indicate the results of 12 images with at least 4 cells per image**. c)** Pictures of human AML cells stained with rabbit anti DDX6 and rabbit anti EDC4 primary antibody were obtained using a Zeiss LSM-880 Airyscan confocal microscope with a 63x magnification lens and using oil as immersion media. White arrows indicate P-body locations.

4) Discussion

P-bodies and also DDX6 have been shown to play a crucial role RNA metabolism (Hubstenberger et al. 2017). It was also shown that DDX6 controls cell fate in a context-dependent manner, giving it unique capabilities among RNA binding proteins (Di Stefano et al. 2019). The role of DDX6 in malignant hematopoiesis has not been studied prior to this work. Therefore, the aim of this thesis was to shed light on the role of DDX6 in human and murine AML cells.

The analysis of two genome-wide CRISPR/Cas9 dropout screens performed in the murine AML cell line CNC and in the normal hematopoietic progenitor cell line HPC-7 indicated that DDX6 could represent a leukemia-specific genetic dependency. Therefore, we first investigated the mRNA and protein levels of DDX6. We found that *DDX6* mRNA levels are higher in murine AML cell than in HPC-7 cells, while protein levels remained comparable. The absence of higher DDX6 protein levels in AML cells could be explained by post-transcriptional regulation, which might prevent an increase of DDX6 protein levels in transformed cells. The upregulation of *DDX6* mRNA levels in the murine AML cell line in comparison to the normal hematopoietic progenitor cell line suggests that transcription of *DDX6* mRNA might be increased during malignant transformation. We next turned our attention to human AML. Using the gene expression profiling interactive analysis (http://gepia.cancer-pku.cn/) online tool we found that *DDX6* expression is highest in human AML patient samples across various cancer types. This was confirmed by qRT-PCR data, which showed that most human AML cell lines we studies showed higher *DDX6* mRNA expression than CD34+ placenta cells. This might indicate that *DDX6* mRNA expression levels are upregulated either during or after malignant transformation. However, we could not detect any significant difference in DDX6 protein levels among the human AML cell lines in comparison to the CD34+ derived placenta cells. Thus, an unknown mechanism of post-transcriptional regulation might prevent an increase in DDX6 protein levels upon malignant transformation. The exact mechanistic details behind the increase of *DDX6* mRNA expression and maintenance of DDX6 protein level remain to be explored.

To follow up and further investigate why *DDX6* expression levels are increased in human AML cells, studies of the accessibility of chromatin structure through ATAC-seq could lead to insights of DDX6 regulation (Buenrostro et al. 2015). To gain insight into the maintenance of

DDX6 protein levels the interference with different post-transcriptional regulatory mechanism might reveal mechanisms that cause the regulation of DDX6 protein levels. Since DDX6 itself is an essential protein for P-body formation and P-bodies are known to retain certain mRNAs from translation, a potential auto-regulatory feedback-loop could be in place. In this loop, DDX6 protein in P-bodies could retain DDX6 mRNA from entering translation to keep DDX6 protein levels constant. To test this hypothesis, DDX6 protein levels could be investigated upon disruption of P-body formation. Furthermore, the inhibition of the lysosomal/autophagy protein degradation pathway by bafilomycin A1 (Newton et al. 2015) or investigating the ubiquitination state of DDX6 via immunoprecipitation followed by western blot analysis might also shed light on the exact mechanism of DDX6 protein homeostasis (Sigismund and Polo 2016).

Since DDX6 turned out as leukemia-specific vulnerability when comparing CNC with HPC-7 cells we aimed to confirm this specific effect in human AML cell lines. We first investigated available CRISPR/Cas9 dropout screening datasets. Both datasets from the DepMap database (https://depmap.org/portal/depmap/; 26 AML cell lines) as well as the dataset generated by Wang and colleagues (Wang et al. 2017) indicated that DDX6 is a strong genetic dependency. When looking at the cancer dependency database DepMap DDX6 not only presented itself as a potential genetic dependency in human AML cells but also in bile duct, breast, lung, pancreatic and colorectal cancer cells. In general, DDX6 showed a negative dependency score in every cancer category present on DepMap. The reason as to why DDX6 seems to a pan-cancer genetic dependency may lie within its function as an RNA helicase and essential P-body protein that has a plethora of different interaction partners while storing and selectively retaining mRNAs in P-bodies. For example, DDX6 has been reported to cause colorectal cancer cells to escape from programmed cell death. DDX6 inhibition led to a proliferative disadvantage via the interference with the Wnt signaling pathway (Lin et al. 2008). A similar mechanism might operate in human AML cells.

We confirmed our findings that DDX6 seems to be a leukemia-specific vulnerability utilizing CRISPR/Cas9 mediated knockout of *DDX6* in a competition-based proliferation assay. Human AML cells harboring a knockout of *DDX6* showed a strong a proliferative disadvantage. Next, we validated these findings by RNA interference. Also the shRNA-mediated knockdown of *DDX6* caused a strong proliferative disadvantage in human AML cells, validating our results from the CRISPR/Cas9-based proliferation assay. Therefore, all our data from experiments

with CRISPR/Cas9-mediated knockout and shRNA-induced knockdown of *DDX6* confirmed the publicly available cancer dependency dataset that DDX6 is a genetic dependency in human AML and that DDX6 is important for AML cell proliferation.

DDX6 has been reported to accumulate in distinct cytoplasmic foci, so called P-bodies in a variety of cell types (Andrei et al. 2005). Furthermore, it has been shown that DDX6 is one of three proteins essential for P-body assembly, the other two being the eIF4E binding protein 4E-T and LSM14A (Ayache et al. 2015). Therefore, we wanted to investigate if the same is true for AML cells. We used immunofluorescence imaging to visualize the cytoplasmic localization of DDX6 together with EDC4, another known marker for P-bodies. We found that DDX6 localized to the cytoplasm accumulated in distinct cytoplasmic foci. Also EDC4 showed a characteristic localization across the entire cytoplasm as well as an accumulation into cytoplasmic foci, presumably P-bodies. When we compared the counts of these cytoplasmic foci stained by DDX6 and EDC4 we found that the average number of foci per cell was similar. This confirms that both DDX6 and EDC4 localize to P-bodies in human and murine AML cell lines.

To gain a deeper understanding of the changes that occur in human AML cell lines upon DDX6 loss we generated a doxycycline-inducible RNA-interference system in which induction of shRNA expression is coupled to the iRFP670 fluorescence marker. We first validated the system by treating cells with doxycycline to induce shRNA expression and measured the percentage of iRFP670 positive cells over time.

We observed a significant time-dependent depletion of cells expressing *DDX6*-targeting shRNAs, indicating the functionality of our system. To measure the kinetics of *DDX6* knockdown, we induced shRNA expression through doxycycline treatment and collected protein and RNA samples at different time points. Protein analysis showed that in MOLM13 cells shDDX6_1 and shDDX6_3 led to a time-dependent depletion of DDX6 protein levels whereas shDDX6_2 showed no effect. In HL60 cells however, only shDDX6_2 led to a depletion of DDX6 protein levels but not shDDX6_1 and shDDX6_3. In MV4:11 cells, DDX6 protein levels were modulated exactly as in in MOLM13, being that shDDX6_1 and shDDX6_3 led to a time-dependent depletion, while shDDX6_2 appeared to have no effect. shDDX6_3 was the only shRNA that led to a depletion in protein signal in THP-1 cells. In all cases the highest depletion of DDX6 protein levels was observed 72 hours post doxycycline induction.

We then tested *DDX6* mRNA levels prior and 72 hours post doxycycline induction. We observed that shDDX6_1 led to a significant decrease of *DDX6* mRNA levels in all cell lines 72 hours after doxycycline induction. These findings suggest that this time point, is best suited to study changes in the transcriptome that occur upon loss of DDX6. The difference in protein level depletion between the different human AML cell lines could be explained by the induction efficiency of shRNAs following doxycycline treatment. Since the protein samples were collected from a population that contained induced and un-induced cells, a lower induction rate could lead to weaker or no depletion of DDX6 protein levels, because the background of un-induced cells would mask the reduction in DDX6 protein levels. Furthermore, DDX6 protein levels are also dependent on protein turnover. If DDX6 protein turnover is slow, 72 hours post induction might be too short to observe representative changes. Another factor influencing protein depletion is the efficiency of shRNA-mediated targeting of DDX6 to cause an efficient knockdown. In addition, some shRNAs might display a higher knockdown efficiency than others. Most likely, the observed differences represent a combinatorial effect of all of the factors mentioned above.

We then wanted to test if DDX6 is essential for the assembly and the maintenance of P-bodies in human AML. We fixed our human acute myeloid leukemia cells prior and 72 hours after knockdown induction and stained them for DDX6 and EDC4. As expected, there was a significant decrease in DDX6 signal intensity upon DDX6 knockdown, which was accompanied by the complete loss of P-bodies. This was also confirmed by the localization pattern of EDC4. This suggests that DDX6 is essential for P-body assembly and maintenance in human AML cells.

Di Stefano et. al described a dual function of DDX6. In some cell types, it drives exit from self-renewal towards differentiation whereas in others DDX6 helps to maintain the self-renewal program and blocks differentiation (Di Stefano et al. 2019). We showed that AML cell lines suffer from a proliferative disadvantage upon DDX6 loss, however we do not know why this is the case. To understand the reason behind this, studies of mRNAs that are associated with DDX6 in the P-bodies and investigations of differentially expressed genes upon DDX6 loss via RNA-seq could be performed. Intersection of these datasets would allow the discovery of genes that might underlie the observed effect. These genes could then be subjected to perturbation to investigate if interference with these genes in the presence of DDX6 would lead

to a similar phenotype we observed upon DDX6 loss. Furthermore, we do not know the exact phenotypic changes that occur in AML cells when DDX6 is lost and their dynamics. It would be important to test if AML blasts undergo terminal differentiation, cell cycle arrest or apoptosis upon DDX6 loss. Combined with the RNA-seq analysis these analyses could help to pinpoint the molecular mechanism underlying the dependence of AML cells on DDX6.

We showed that DDX6 is essential for the formation of P-bodies in human AML cell lines. The role of DDX6 in P-bodies has not yet been extensively studied apart from its essentiality in P-body formation (Ayache et al. 2015). As DDX6 is an RNA helicase its role could be binding and changing the confirmation of selective mRNAs to either retain them in P-bodies or enable them to re-enter translation. However, the RNA helicase-dependent role of DDX6 during malignant transformation is yet to be uncovered. The investigation of a catalytically inactive mutant of DDX6 that lacks its helicase capabilities could shed light on this question. RNA-seq analysis could be performed to test if the absence of DDX6's enzymatic function would lead to a similar pattern of gene expression as the absence of DDX6.

Furthermore, to this date it is not known if the role of DDX6 in cancer and AML is restricted to P-bodies or if cytoplasmic DDX6 also has a function. To test this, one could inhibit P-body formation like it has been described recently by a small molecule inhibitor which inhibits the association of DDX6 with 4E-T thereby preventing formation of P-bodies (Kami et al. 2022) and then check if the phenotypical changes resemble those that are observed upon DDX6 loss. Taken together, further work needs to be performed to fully understand the molecular mechanisms underlie the dependency of AML cells on DDX6.

In conclusion, our findings identified DDX6 – an RNA-binding protein localized in the cytoplasmic processing bodies (P-bodies) - as a novel genetic vulnerability in AML. DDX6 expression is upregulated in leukemia compared to healthy, untransformed cells as well as in samples from healthy donors. Furthermore, we demonstrated the importance of DDX6 for the maintenance of the integrity of P-bodies, as its loss led to their complete disappearance in AML cells. Taken together, these findings deepen our understanding of the role of DDX6 during malignant hematopoiesis and open the door to potential targeted therapies against DDX6 like it is the case for DDX3, which has been postulated as a potential targeted therapy in lung cancer by a small molecular inhibitor, (Bol, Xie, and Raman 2015) to induce AML blast cell

death and circumvent chemotherapeutic treatment. However, for this a functional small molecule inhibitor for DDX6 needs to be found.

5) Acknowledgments:

First of all, I would like to thank Prof. Florian Grebien for giving me the opportunity to perform my master thesis in his lab and for the feedback on my work. I am very grateful for all the things I was able to learn and greatly enjoyed his supervision while working on this project.

Next, I want to thank Ludovica Proietti for trusting me to work with her on this project. I am forever grateful that she shared her experience and knowledge with me and I am thankful for all the advice and support she gave me, she was the best supervisor anyone could wish for.

Lastly, I want to thank everyone else in the lab as for providing such a welcoming and collaborative work environment.

6) Abstract:

Summary: The Role of the DEAD box RNA helicase DDX6 in normal and malignant hematopoiesis

Master Thesis: Bernhard Alber, Matr.Nr: 01635001

Supervisor: Univ.-Prof. Dr.rer.nat Florian Grebien

Proposed Reviewers: Dr. Karoline Kollmann (Institute for Pharmacology and Toxicology)

mRNAs interact with RNA-binding proteins (RBPs) as well as with other coding and non-coding RNAs in the context of ribonucleoprotein complexes (RNPs). RBPs are important in nearly all post-transcriptional processes of RNA metabolism, including splicing, alternative polyadenylation, localization, surveillance, decay and translation. RNA-binding proteins are aberrantly expressed in various cancer types, including acute myeloid leukemia (AML), which is a neoplasm of the myeloid blood lineage, causing aberrant expansion of immature cells at the expense of mature cell production. Processing bodies (P-Bodies) are membraneless cytoplasmic foci containing mRNPs associated with translational repression and mRNA decay machineries. DDX6 is a member of the DEAD-box RNA helicase family which is essential for the assembly and maintenance of P-bodies in eukaryotic cells. Furthermore, it has been shown that DDX6 is able to control cell fate in a context-dependent manner. This work aims to elucidate the role of DDX6 in malignant hematopoiesis, since its role in controlling differentiation vs. self-renewal has not been studied in AML. Analysis of publicly available gene expression databases revealed that DDX6 levels are higher in cancer cells than in healthy cells. Western blot and RT-qPCR analysis confirmed that DDX6 protein and mRNA levels are elevated in mouse and human AML cell lines and patient samples compared to untransformed hematopoietic progenitor cells. CRISPR/Cas9-mediated gene knockout and doxycycline-inducible shRNA-mediated knockdown showed that DDX6 is essential for AML cell proliferation. Furthermore, DDX6 loss caused the dissolution of P-bodies in AML cells, confirming its requirement for their assembly and maintenance. Together, this work contributes to a deeper understanding of the function of DDX6 during malignant hematopoiesis.

7) References:

https://www.alfa-leukemia.org/en/aml#:~:text=AML%20is%20a%20blood%20cancer,production%2C%20called%20bone%20marrow%20failure.

Agrawal, N., P. V. Dasaradhi, A. Mohmmed, P. Malhotra, R. K. Bhatnagar, and S. K. Mukherjee. 2003. 'RNA interference: biology, mechanism, and applications', *Microbiol Mol Biol Rev*, 67: 657-85.

Aizer, A., A. Kalo, P. Kafri, A. Shraga, R. Ben-Yishay, A. Jacob, N. Kinor, and Y. Shav-Tal. 2014. 'Quantifying mRNA targeting to P-bodies in living human cells reveals their dual role in mRNA decay and storage', *J Cell Sci*, 127: 4443-56.

An, X., A. K. Tiwari, Y. Sun, P. R. Ding, C. R. Ashby, Jr., and Z. S. Chen. 2010. 'BCR-ABL tyrosine kinase inhibitors in the treatment of Philadelphia chromosome positive chronic myeloid leukemia: a review', *Leuk Res*, 34: 1255-68.

Andrei, M. A., D. Ingelfinger, R. Heintzmann, T. Achsel, R. Rivera-Pomar, and R. Luhrmann. 2005. 'A role for eIF4E and eIF4E-transporter in targeting mRNPs to mammalian processing bodies', *RNA*, 11: 717-27.

Ayache, J., M. Benard, M. Ernoult-Lange, N. Minshall, N. Standart, M. Kress, and D. Weil. 2015. 'P-body assembly requires DDX6 repression complexes rather than decay or Ataxin2/2L complexes', *Mol Biol Cell*, 26: 2579-95.

Azuma-Mukai, A., H. Oguri, T. Mituyama, Z. R. Qian, K. Asai, H. Siomi, and M. C. Siomi. 2008. 'Characterization of endogenous human Argonautes and their miRNA partners in RNA silencing', *Proc Natl Acad Sci U S A*, 105: 7964-9.

Bajaj, J., M. Hamilton, Y. Shima, K. Chambers, K. Spinler, E. L. Van Nostrand, B. A. Yee, S. M. Blue, M. Chen, D. Rizzeri, C. Chuah, V. G. Oehler, H. E. Broome, R. Sasik, J. Scott-Browne, A. Rao, G. W. Yeo, and T. Reya. 2020. 'An in vivo genome-wide CRISPR screen identifies the RNA-binding protein Staufen2 as a key regulator of myeloid leukemia', *Nat Cancer*, 1: 410-22.

Ben-Neriah, Y., G. Q. Daley, A. M. Mes-Masson, O. N. Witte, and D. Baltimore. 1986. 'The chronic myelogenous leukemia-specific P210 protein is the product of the bcr/abl hybrid gene', *Science*, 233: 212-4.

Benjamin, D., and C. Moroni. 2007. 'mRNA stability and cancer: an emerging link?', *Expert Opin Biol Ther*, 7: 1515-29.

Boettcher, M., and M. T. McManus. 2015. 'Choosing the Right Tool for the Job: RNAi, TALEN, or CRISPR', *Mol Cell*, 58: 575-85.

Bol, G. M., M. Xie, and V. Raman. 2015. 'DDX3, a potential target for cancer treatment', *Mol Cancer*, 14: 188.

Bortz, E., L. Westera, J. Maamary, J. Steel, R. A. Albrecht, B. Manicassamy, G. Chase, L. Martinez-Sobrido, M. Schwemmle, and A. Garcia-Sastre. 2011. 'Host- and strain-specific regulation of influenza virus polymerase activity by interacting cellular proteins', *mBio*, 2.

Boutros, M., and J. Ahringer. 2008. 'The art and design of genetic screens: RNA interference', *Nat Rev Genet*, 9: 554-66.

Buddika, K., Y. T. Huang, I. S. Ariyapala, A. Butrum-Griffith, S. A. Norrell, A. M. O'Connor, V. K. Patel, S. A. Rector, M. Slovan, M. Sokolowski, Y. Kato, A. Nakamura, and N. S. Sokol. 2022. 'Coordinated repression of pro-differentiation genes via P-bodies and transcription maintains Drosophila intestinal stem cell identity', *Curr Biol*, 32: 386-97 e6.

Buenrostro, J. D., B. Wu, H. Y. Chang, and W. J. Greenleaf. 2015. 'ATAC-seq: A Method for Assaying Chromatin Accessibility Genome-Wide', *Curr Protoc Mol Biol*, 109: 21 29 1-21 29 9.

Cesana, M., D. Cacchiarelli, I. Legnini, T. Santini, O. Sthandier, M. Chinappi, A. Tramontano, and I. Bozzoni. 2011. 'A long noncoding RNA controls muscle differentiation by functioning as a competing endogenous RNA', *Cell*, 147: 358-69.

Chan, S. M., D. Thomas, M. R. Corces-Zimmerman, S. Xavy, S. Rastogi, W. J. Hong, F. Zhao, B. C. Medeiros, D. A. Tyvoll, and R. Majeti. 2015. 'Isocitrate dehydrogenase 1 and 2 mutations induce BCL-2 dependence in acute myeloid leukemia', *Nat Med*, 21: 178-84.

Corsini, N. S., A. M. Peer, P. Moeseneder, M. Roiuk, T. R. Burkard, H. C. Theussl, I. Moll, and J. A. Knoblich. 2018. 'Coordinated Control of mRNA and rRNA Processing Controls Embryonic Stem Cell Pluripotency and Differentiation', *Cell Stem Cell*, 22: 543-58 e12.

Cougot, N., S. Babajko, and B. Seraphin. 2004. 'Cytoplasmic foci are sites of mRNA decay in human cells', *J Cell Biol*, 165: 31-40.

Dang, L., D. W. White, S. Gross, B. D. Bennett, M. A. Bittinger, E. M. Driggers, V. R. Fantin, H. G. Jang, S. Jin, M. C. Keenan, K. M. Marks, R. M. Prins, P. S. Ward, K. E. Yen, L. M. Liau, J. D. Rabinowitz, L. C. Cantley, C. B. Thompson, M. G. Vander Heiden, and S. M. Su. 2009. 'Cancer-associated IDH1 mutations produce 2-hydroxyglutarate', *Nature*, 462: 739-44.

Daver, N., R. F. Schlenk, N. H. Russell, and M. J. Levis. 2019. 'Targeting FLT3 mutations in AML: review of current knowledge and evidence', *Leukemia*, 33: 299-312.

Daver, N., A. H. Wei, D. A. Pollyea, A. T. Fathi, P. Vyas, and C. D. DiNardo. 2020. 'New directions for emerging therapies in acute myeloid leukemia: the next chapter', *Blood Cancer J*, 10: 107.

Dawson, M. I., and Z. Xia. 2012. 'The retinoid X receptors and their ligands', *Biochim Biophys Acta*, 1821: 21-56.

De Braekeleer, E., N. Douet-Guilbert, and M. De Braekeleer. 2014. 'RARA fusion genes in acute promyelocytic leukemia: a review', *Expert Rev Hematol*, 7: 347-57.

De Kouchkovsky, I., and M. Abdul-Hay. 2016. ''Acute myeloid leukemia: a comprehensive review and 2016 update'', *Blood Cancer J*, 6: e441.

Di Stefano, B., E. C. Luo, C. Haggerty, S. Aigner, J. Charlton, J. Brumbaugh, F. Ji, I. Rabano Jimenez, K. J. Clowers, A. J. Huebner, K. Clement, I. Lipchina, M. A. C. de Kort, A. Anselmo, J. Pulice, M. F. M. Gerli, H. Gu, S. P. Gygi, R. I. Sadreyev, A. Meissner, G. W. Yeo, and K. Hochedlinger. 2019. 'The RNA Helicase DDX6 Controls Cellular Plasticity by Modulating P-Body Homeostasis', *Cell Stem Cell*, 25: 622-38 e13.

DiNardo, C. D., and J. E. Cortes. 2016. 'Mutations in AML: prognostic and therapeutic implications', *Hematology Am Soc Hematol Educ Program*, 2016: 348-55.

Doudna, J. A., and E. Charpentier. 2014. 'Genome editing. The new frontier of genome engineering with CRISPR-Cas9', *Science*, 346: 1258096.

Eulalio, A., I. Behm-Ansmant, and E. Izaurralde. 2007. 'P bodies: at the crossroads of post-transcriptional pathways', *Nat Rev Mol Cell Biol*, 8: 9-22.

Figueroa, M. E., O. Abdel-Wahab, C. Lu, P. S. Ward, J. Patel, A. Shih, Y. Li, N. Bhagwat, A. Vasanthakumar, H. F. Fernandez, M. S. Tallman, Z. Sun, K. Wolniak, J. K. Peeters, W. Liu, S. E. Choe, V. R. Fantin, E. Paietta, B. Lowenberg, J. D. Licht, L. A. Godley, R. Delwel, P. J. Valk, C. B. Thompson, R. L. Levine, and A. Melnick. 2010. 'Leukemic IDH1 and IDH2 mutations result in a hypermethylation phenotype, disrupt TET2 function, and impair hematopoietic differentiation', *Cancer Cell*, 18: 553-67.

Fraga de Andrade, I., C. Mehta, and E. H. Bresnick. 2020. 'Post-transcriptional control of cellular differentiation by the RNA exosome complex', *Nucleic Acids Res*, 48: 11913-28.

Fu, X. D., and M. Ares, Jr. 2014. 'Context-dependent control of alternative splicing by RNA-binding proteins', *Nat Rev Genet*, 15: 689-701.

Gaillard, C., T. A. Tokuyasu, G. Rosen, J. Sotzen, A. Vitaliano-Prunier, R. Roy, E. Passegue, H. de The, M. E. Figueroa, and S. C. Kogan. 2015. 'Transcription and methylation analyses of preleukemic promyelocytes indicate a dual role for PML/RARA in leukemia initiation', *Haematologica*, 100: 1064-75.

Grafone, T., M. Palmisano, C. Nicci, and S. Storti. 2012. 'An overview on the role of FLT3-tyrosine kinase receptor in acute myeloid leukemia: biology and treatment', *Oncol Rev*, 6: e8.

Han, Y., A. Ye, Y. Zhang, Z. Cai, W. Wang, L. Sun, S. Jiang, J. Wu, K. Yu, and S. Zhang. 2015. 'Musashi-2 Silencing Exerts Potent Activity against Acute Myeloid Leukemia and Enhances Chemosensitivity to Daunorubicin', *PLoS One*, 10: e0136484.

Heyes, E., L. Schmidt, G. Manhart, T. Eder, L. Proietti, and F. Grebien. 2021. 'Identification of gene targets of mutant C/EBPalpha reveals a critical role for MSI2 in CEBPA-mutated AML', *Leukemia*, 35: 2526-38.

Hopkins, T. G., M. Mura, H. A. Al-Ashtal, R. M. Lahr, N. Abd-Latip, K. Sweeney, H. Lu, J. Weir, M. El-Bahrawy, J. H. Steel, S. Ghaem-Maghami, E. O. Aboagye, A. J. Berman, and S. P. Blagden. 2016. 'The RNA-binding protein LARP1 is a post-transcriptional regulator of survival and tumorigenesis in ovarian cancer', *Nucleic Acids Res*, 44: 1227-46.

Hsu, K. S., and H. Y. Kao. 2018. 'PML: Regulation and multifaceted function beyond tumor suppression', *Cell Biosci*, 8: 5.

Hu, T., N. Chitnis, D. Monos, and A. Dinh. 2021. 'Next-generation sequencing technologies: An overview', *Hum Immunol*, 82: 801-11.

Hubstenberger, A., M. Courel, M. Benard, S. Souquere, M. Ernoult-Lange, R. Chouaib, Z. Yi, J. B. Morlot, A. Munier, M. Fradet, M. Daunesse, E. Bertrand, G. Pierron, J. Mozziconacci, M. Kress, and D. Weil. 2017. 'P-Body Purification Reveals the Condensation of Repressed mRNA Regulons', *Mol Cell*, 68: 144-57 e5.

Hwang, S. M. 2020. 'Classification of acute myeloid leukemia', *Blood Res*, 55: S1-S4.

Hyman, A. A., C. A. Weber, and F. Julicher. 2014. 'Liquid-liquid phase separation in biology', *Annu Rev Cell Dev Biol*, 30: 39-58.

Iqbal, N., and N. Iqbal. 2014. 'Imatinib: a breakthrough of targeted therapy in cancer', *Chemother Res Pract*, 2014: 357027.

Issa, G. C., and C. D. DiNardo. 2021. 'Acute myeloid leukemia with IDH1 and IDH2 mutations: 2021 treatment algorithm', *Blood Cancer J*, 11: 107.

Ito, K., A. Carracedo, D. Weiss, F. Arai, U. Ala, D. E. Avigan, Z. T. Schafer, R. M. Evans, T. Suda, C. H. Lee, and P. P. Pandolfi. 2012. 'A PML-PPAR-delta pathway for fatty acid oxidation regulates hematopoietic stem cell maintenance', *Nat Med*, 18: 1350-8.

Jangra, R. K., M. Yi, and S. M. Lemon. 2010. 'DDX6 (Rck/p54) is required for efficient hepatitis C virus replication but not for internal ribosome entry site-directed translation', *J Virol*, 84: 6810-24.

Kale, J., E. J. Osterlund, and D. W. Andrews. 2018. 'BCL-2 family proteins: changing partners in the dance towards death', *Cell Death Differ*, 25: 65-80.

Kamashev, D., D. Vitoux, and H. De The. 2004. 'PML-RARA-RXR oligomers mediate retinoid and rexinoid/cAMP cross-talk in acute promyelocytic leukemia cell differentiation', *J Exp Med*, 199: 1163-74.

Kami, D., T. Ishizaki, T. Taya, A. Katoh, H. Kouji, and S. Gojo. 2022. 'A novel mRNA decay inhibitor abolishes pathophysiological cellular transition', *Cell Death Discov*, 8: 278.

Kami, D., T. Kitani, A. Nakamura, N. Wakui, R. Mizutani, M. Ohue, F. Kametani, N. Akimitsu, and S. Gojo. 2018. 'The DEAD-box RNA-binding protein DDX6 regulates parental RNA decay for cellular reprogramming to pluripotency', *PLoS One*, 13: e0203708.

Kang, D., Y. Lee, and J. S. Lee. 2020. 'RNA-Binding Proteins in Cancer: Functional and Therapeutic Perspectives', *Cancers (Basel)*, 12.

Kantarjian, H., T. Kadia, C. DiNardo, N. Daver, G. Borthakur, E. Jabbour, G. Garcia-Manero, M. Konopleva, and F. Ravandi. 2021. 'Acute myeloid leukemia: current progress and future directions', *Blood Cancer J*, 11: 41.

Kassim, A. A., and B. N. Savani. 2017. 'Hematopoietic stem cell transplantation for acute myeloid leukemia: A review', *Hematol Oncol Stem Cell Ther*, 10: 245-51.

Kharas, M. G., C. J. Lengner, F. Al-Shahrour, L. Bullinger, B. Ball, S. Zaidi, K. Morgan, W. Tam, M. Paktinat, R. Okabe, M. Gozo, W. Einhorn, S. W. Lane, C. Scholl, S. Frohling, M. Fleming, B. L. Ebert, D. G. Gilliland, R. Jaenisch, and G. Q. Daley. 2010. 'Musashi-2 regulates normal hematopoiesis and promotes aggressive myeloid leukemia', *Nat Med*, 16: 903-8.

Kim, M. Y., J. Hur, and S. Jeong. 2009. 'Emerging roles of RNA and RNA-binding protein network in cancer cells', *BMB Rep*, 42: 125-30.

King, C. E., M. Cuatrecasas, A. Castells, A. R. Sepulveda, J. S. Lee, and A. K. Rustgi. 2011. 'LIN28B promotes colon cancer progression and metastasis', *Cancer Res*, 71: 4260-8.

Lin, A., and J. M. Sheltzer. 2020. 'Discovering and validating cancer genetic dependencies: approaches and pitfalls', *Nat Rev Genet*, 21: 671-82.

Lin, F., R. Wang, J. J. Shen, X. Wang, P. Gao, K. Dong, and H. Z. Zhang. 2008. 'Knockdown of RCK/p54 expression by RNAi inhibits proliferation of human colorectal cancer cells in vitro and in vivo', *Cancer Biol Ther*, 7: 1669-76.

Linder, P., and E. Jankowsky. 2011. 'From unwinding to clamping - the DEAD box RNA helicase family', *Nat Rev Mol Cell Biol*, 12: 505-16.

Ling, S. H., C. J. Decker, M. A. Walsh, M. She, R. Parker, and H. Song. 2008. 'Crystal structure of human Edc3 and its functional implications', *Mol Cell Biol*, 28: 5965-76.

Liquori, A., M. Ibanez, C. Sargas, M. A. Sanz, E. Barragan, and J. Cervera. 2020. 'Acute Promyelocytic Leukemia: A Constellation of Molecular Events around a Single PML-RARA Fusion Gene', *Cancers (Basel)*, 12.

Liu, L., A. Vujovic, N. P. Deshpande, S. Sathe, G. Anande, H. T. T. Chen, J. Xu, M. D. Minden, G. W. Yeo, A. Unnikrishnan, K. J. Hope, and Y. Lu. 2022. 'The splicing factor RBM17 drives leukemic stem cell maintenance by evading nonsense-mediated decay of pro-leukemic factors', *Nat Commun*, 13: 3833.

Lo-Coco, F., G. Avvisati, M. Vignetti, C. Thiede, S. M. Orlando, S. Iacobelli, F. Ferrara, P. Fazi, L. Cicconi, E. Di Bona, G. Specchia, S. Sica, M. Divona, A. Levis, W. Fiedler, E. Cerqui, M. Breccia, G. Fioritoni, H. R. Salih, M. Cazzola, L. Melillo, A. M. Carella, C. H. Brandts, E. Morra, M. von Lilienfeld-Toal, B. Hertenstein, M. Wattad, M. Lubbert, M. Hanel, N. Schmitz, H. Link, M. G. Kropp, A. Rambaldi, G. La Nasa, M. Luppi, F. Ciceri, O. Finizio, A. Venditti, F. Fabbiano, K. Dohner, M. Sauer, A. Ganser, S. Amadori, F. Mandelli, H. Dohner, G. Ehninger, R. F. Schlenk, U. Platzbecker, dell'Adulto Gruppo Italiano Malattie Ematologiche, Group German-Austrian Acute Myeloid Leukemia Study, and Leukemia Study Alliance. 2013. 'Retinoic acid and arsenic trioxide for acute promyelocytic leukemia', *N Engl J Med*, 369: 111-21.

Lorgeoux, R. P., Q. Pan, Y. Le Duff, and C. Liang. 2013. 'DDX17 promotes the production of infectious HIV-1 particles through modulating viral RNA packaging and translation frameshift', *Virology*, 443: 384-92.

Lukong, K. E., K. W. Chang, E. W. Khandjian, and S. Richard. 2008. 'RNA-binding proteins in human genetic disease', *Trends Genet*, 24: 416-25.

Lumb, J. H., Q. Li, L. M. Popov, S. Ding, M. T. Keith, B. D. Merrill, H. B. Greenberg, J. B. Li, and J. E. Carette. 2017. 'DDX6 Represses Aberrant Activation of Interferon-Stimulated Genes', *Cell Rep*, 20: 819-31.

Ma, Z., R. Moore, X. Xu, and G. N. Barber. 2013. 'DDX24 negatively regulates cytosolic RNA-mediated innate immune signaling', *PLoS Pathog*, 9: e1003721.

Marcel, V., F. Catez, C. M. Berger, E. Perrial, A. Plesa, X. Thomas, E. Mattei, S. Hayette, P. Saintigny, P. Bouvet, J. J. Diaz, and C. Dumontet. 2017. 'Expression Profiling of Ribosome Biogenesis Factors Reveals Nucleolin as a Novel Potential Marker to Predict Outcome in AML Patients', *PLoS One*, 12: e0170160.

Martens, J. H., and H. G. Stunnenberg. 2010. 'The molecular signature of oncofusion proteins in acute myeloid leukemia', *FEBS Lett*, 584: 2662-9.

Mazzoni, C., and C. Falcone. 2011. 'mRNA stability and control of cell proliferation', *Biochem Soc Trans*, 39: 1461-5.

McCubrey, J. A., L. S. Steelman, W. H. Chappell, S. L. Abrams, E. W. Wong, F. Chang, B. Lehmann, D. M. Terrian, M. Milella, A. Tafuri, F. Stivala, M. Libra, J. Basecke, C. Evangelisti, A. M. Martelli, and R. A. Franklin. 2007. 'Roles of the Raf/MEK/ERK

pathway in cell growth, malignant transformation and drug resistance', *Biochim Biophys Acta*, 1773: 1263-84.

Minuesa, G., S. K. Albanese, W. Xie, Y. Kazansky, D. Worroll, A. Chow, A. Schurer, S. M. Park, C. Z. Rotsides, J. Taggart, A. Rizzi, L. N. Naden, T. Chou, S. Gourkanti, D. Cappel, M. C. Passarelli, L. Fairchild, C. Adura, J. F. Glickman, J. Schulman, C. Famulare, M. Patel, J. K. Eibl, G. M. Ross, S. Bhattacharya, D. S. Tan, C. S. Leslie, T. Beuming, D. J. Patel, Y. Goldgur, J. D. Chodera, and M. G. Kharas. 2019. 'Small-molecule targeting of MUSASHI RNA-binding activity in acute myeloid leukemia', *Nat Commun*, 10: 2691.

Nasr, R., V. Lallemand-Breitenbach, J. Zhu, M. C. Guillemin, and H. de The. 2009. 'Therapy-induced PML/RARA proteolysis and acute promyelocytic leukemia cure', *Clin Cancer Res*, 15: 6321-6.

Newton, P. T., K. K. Vuppalapati, T. Bouderlique, and A. S. Chagin. 2015. 'Pharmacological inhibition of lysosomes activates the MTORC1 signaling pathway in chondrocytes in an autophagy-independent manner', *Autophagy*, 11: 1594-607.

Nicklas, S., S. Okawa, A. L. Hillje, L. Gonzalez-Cano, A. Del Sol, and J. C. Schwamborn. 2015. 'The RNA helicase DDX6 regulates cell-fate specification in neural stem cells via miRNAs', *Nucleic Acids Res*, 43: 2638-54.

Nunez, R. D., M. Budt, S. Saenger, K. Paki, U. Arnold, A. Sadewasser, and T. Wolff. 2018. 'The RNA Helicase DDX6 Associates with RIG-I to Augment Induction of Antiviral Signaling', *Int J Mol Sci*, 19.

Pacini, C., J. M. Dempster, I. Boyle, E. Goncalves, H. Najgebauer, E. Karakoc, D. van der Meer, A. Barthorpe, H. Lightfoot, P. Jaaks, J. M. McFarland, M. J. Garnett, A. Tsherniak, and F. Iorio. 2021. 'Integrated cross-study datasets of genetic dependencies in cancer', *Nat Commun*, 12: 1661.

Paplomata, E., R. Nahta, and R. M. O'Regan. 2015. 'Systemic therapy for early-stage HER2-positive breast cancers: time for a less-is-more approach?', *Cancer*, 121: 517-26.

Parker, R., and U. Sheth. 2007. 'P bodies and the control of mRNA translation and degradation', *Mol Cell*, 25: 635-46.

Paronetto, M. P., T. Achsel, A. Massiello, C. E. Chalfant, and C. Sette. 2007. 'The RNA-binding protein Sam68 modulates the alternative splicing of Bcl-x', *J Cell Biol*, 176: 929-39.

Pelcovits, A., and R. Niroula. 2020. 'Acute Myeloid Leukemia: A Review', *R I Med J (2013)*, 103: 38-40.

Pereira, B., M. Billaud, and R. Almeida. 2017. 'RNA-Binding Proteins in Cancer: Old Players and New Actors', *Trends Cancer*, 3: 506-28.

Prieto, C., D. T. T. Nguyen, Z. Liu, J. Wheat, A. Perez, S. Gourkanti, T. Chou, E. Barin, A. Velleca, T. Rohwetter, A. Chow, J. Taggart, A. M. Savino, K. Hoskova, M. Dhodapkar, A. Schurer, T. S. Barlowe, L. P. Vu, C. Leslie, U. Steidl, R. Rabadan, and M. G. Kharas. 2021. 'Transcriptional control of CBX5 by the RNA binding proteins RBMX and RBMXL1 maintains chromatin state in myeloid leukemia', *Nat Cancer*, 2: 741-57.

Rocak, S., and P. Linder. 2004. 'DEAD-box proteins: the driving forces behind RNA metabolism', *Nat Rev Mol Cell Biol*, 5: 232-41.

Samra, B., M. Konopleva, A. Isidori, N. Daver, and C. DiNardo. 2020. 'Venetoclax-Based Combinations in Acute Myeloid Leukemia: Current Evidence and Future Directions', *Front Oncol*, 10: 562558.

Schambach, A., M. Galla, U. Modlich, E. Will, S. Chandra, L. Reeves, M. Colbert, D. A. Williams, C. von Kalle, and C. Baum. 2006. 'Lentiviral vectors pseudotyped with murine ecotropic envelope: increased biosafety and convenience in preclinical research', *Exp Hematol*, 34: 588-92.

Schuschel, K., M. Helwig, S. Huttelmaier, D. Heckl, J. H. Klusmann, and J. I. Hoell. 2020. 'RNA-Binding Proteins in Acute Leukemias', *Int J Mol Sci*, 21.

Sfakianos, A. P., A. J. Whitmarsh, and M. P. Ashe. 2016. 'Ribonucleoprotein bodies are phased in', *Biochem Soc Trans*, 44: 1411-16.

Sharma, S. V., and J. Settleman. 2007. 'Oncogene addiction: setting the stage for molecularly targeted cancer therapy', *Genes Dev*, 21: 3214-31.

Shen, N., F. Yan, J. Pang, L. C. Wu, A. Al-Kali, M. R. Litzow, and S. Liu. 2014. 'A nucleolin-DNMT1 regulatory axis in acute myeloid leukemogenesis', *Oncotarget*, 5: 5494-509.

Sheth, U., and R. Parker. 2003. 'Decapping and decay of messenger RNA occur in cytoplasmic processing bodies', *Science*, 300: 805-8.

Siegel, R. L., K. D. Miller, H. E. Fuchs, and A. Jemal. 2021. 'Cancer Statistics, 2021', *CA Cancer J Clin*, 71: 7-33.

Sigismund, S., and S. Polo. 2016. 'Strategies to Detect Endogenous Ubiquitination of a Target Mammalian Protein', *Methods Mol Biol*, 1449: 143-51.

Smith, C. C. 2019. 'The growing landscape of FLT3 inhibition in AML', *Hematology Am Soc Hematol Educ Program*, 2019: 539-47.

Standart, N., and D. Weil. 2018. 'P-Bodies: Cytosolic Droplets for Coordinated mRNA Storage', *Trends Genet*, 34: 612-26.

Tajrishi, M. M., R. Tuteja, and N. Tuteja. 2011. 'Nucleolin: The most abundant multifunctional phosphoprotein of nucleolus', *Commun Integr Biol*, 4: 267-75.

Taniguchi, K., A. Iwatsuki, N. Sugito, H. Shinohara, Y. Kuranaga, Y. Oshikawa, T. Tajirika, M. Futamura, K. Yoshida, K. Uchiyama, and Y. Akao. 2018. 'Oncogene RNA helicase DDX6 promotes the process of c-Myc expression in gastric cancer cells', *Mol Carcinog*, 57: 579-89.

Taschuk, F., and S. Cherry. 2020. 'DEAD-Box Helicases: Sensors, Regulators, and Effectors for Antiviral Defense', *Viruses*, 12.

van Dijk, E., N. Cougot, S. Meyer, S. Babajko, E. Wahle, and B. Seraphin. 2002. 'Human Dcp2: a catalytically active mRNA decapping enzyme located in specific cytoplasmic structures', *EMBO J*, 21: 6915-24.

Vellky, J. E., S. T. McSweeney, E. A. Ricke, and W. A. Ricke. 2020. 'RNA-binding protein DDX3 mediates posttranscriptional regulation of androgen receptor: A mechanism of castration resistance', *Proc Natl Acad Sci U S A*, 117: 28092-101.

Vo, D. T., D. Subramaniam, M. Remke, T. L. Burton, P. J. Uren, J. A. Gelfond, R. de Sousa Abreu, S. C. Burns, M. Qiao, U. Suresh, A. Korshunov, A. M. Dubuc, P. A. Northcott, A. D. Smith, S. M. Pfister, M. D. Taylor, S. C. Janga, S. Anant, C. Vogel,

and L. O. Penalva. 2012. 'The RNA-binding protein Musashi1 affects medulloblastoma growth via a network of cancer-related genes and is an indicator of poor prognosis', *Am J Pathol*, 181: 1762-72.

Vu, L. P., C. Prieto, E. M. Amin, S. Chhangawala, A. Krivtsov, M. N. Calvo-Vidal, T. Chou, A. Chow, G. Minuesa, S. M. Park, T. S. Barlowe, J. Taggart, P. Tivnan, R. P. Deering, L. P. Chu, J. A. Kwon, C. Meydan, J. Perales-Paton, A. Arshi, M. Gonen, C. Famulare, M. Patel, E. Paietta, M. S. Tallman, Y. Lu, J. Glass, F. E. Garret-Bakelman, A. Melnick, R. Levine, F. Al-Shahrour, M. Jaras, N. Hacohen, A. Hwang, R. Garippa, C. J. Lengner, S. A. Armstrong, L. Cerchietti, G. S. Cowley, D. Root, J. Doench, C. Leslie, B. L. Ebert, and M. G. Kharas. 2017. 'Functional screen of MSI2 interactors identifies an essential role for SYNCRIP in myeloid leukemia stem cells', *Nat Genet*, 49: 866-75.

Wang, E., S. X. Lu, A. Pastore, X. Chen, J. Imig, S. Chun-Wei Lee, K. Hockemeyer, Y. E. Ghebrechristos, A. Yoshimi, D. Inoue, M. Ki, H. Cho, L. Bitner, A. Kloetgen, K. T. Lin, T. Uehara, T. Owa, R. Tibes, A. R. Krainer, O. Abdel-Wahab, and I. Aifantis. 2019. 'Targeting an RNA-Binding Protein Network in Acute Myeloid Leukemia', *Cancer Cell*, 35: 369-84 e7.

Wang, G., Y. Tian, Q. Hu, X. Xiao, and S. Chen. 2018. 'PML/RARa blocks the differentiation and promotes the proliferation of acute promyelocytic leukemia through activating MYB expression by transcriptional and epigenetic regulation mechanisms', *J Cell Biochem*.

Wang, T., H. Yu, N. W. Hughes, B. Liu, A. Kendirli, K. Klein, W. W. Chen, E. S. Lander, and D. M. Sabatini. 2017. 'Gene Essentiality Profiling Reveals Gene Networks and Synthetic Lethal Interactions with Oncogenic Ras', *Cell*, 168: 890-903 e15.

Wang, Y., M. Arribas-Layton, Y. Chen, J. Lykke-Andersen, and G. L. Sen. 2015. 'DDX6 Orchestrates Mammalian Progenitor Function through the mRNA Degradation and Translation Pathways', *Mol Cell*, 60: 118-30.

Ward, A. M., K. Bidet, A. Yinglin, S. G. Ler, K. Hogue, W. Blackstock, J. Gunaratne, and M. A. Garcia-Blanco. 2011. 'Quantitative mass spectrometry of DENV-2 RNA-interacting proteins reveals that the DEAD-box RNA helicase DDX6 binds the DB1 and DB2 3' UTR structures', *RNA Biol*, 8: 1173-86.

Wurth, L. 2012. 'Versatility of RNA-Binding Proteins in Cancer', *Comp Funct Genomics*, 2012: 178525.

Xu, A., N. Zhang, J. Cao, H. Zhu, B. Yang, Q. He, X. Shao, and M. Ying. 2020. 'Post-translational modification of retinoic acid receptor alpha and its roles in tumor cell differentiation', *Biochem Pharmacol*, 171: 113696.

Yoshida, H., H. Ichikawa, Y. Tagata, T. Katsumoto, K. Ohnishi, Y. Akao, T. Naoe, P. P. Pandolfi, and I. Kitabayashi. 2007. 'PML-retinoic acid receptor alpha inhibits PML IV enhancement of PU.1-induced C/EBPepsilon expression in myeloid differentiation', *Mol Cell Biol*, 27: 5819-34.

Zheng, D., N. Ezzeddine, C. Y. Chen, W. Zhu, X. He, and A. B. Shyu. 2008. 'Deadenylation is prerequisite for P-body formation and mRNA decay in mammalian cells', *J Cell Biol*, 182: 89-101.

Zuber, J., K. McJunkin, C. Fellmann, L. E. Dow, M. J. Taylor, G. J. Hannon, and S. W. Lowe. 2011. 'Toolkit for evaluating genes required for proliferation and survival using tetracycline-regulated RNAi', *Nat Biotechnol*, 29: 79-83.

Zuber, J., A. R. Rappaport, W. Luo, E. Wang, C. Chen, A. V. Vaseva, J. Shi, S. Weissmueller, C. Fellmann, M. J. Taylor, M. Weissenboeck, T. G. Graeber, S. C. Kogan, C. R. Vakoc, and S. W. Lowe. 2011. 'An integrated approach to dissecting oncogene addiction implicates a Myb-coordinated self-renewal program as essential for leukemia maintenance', *Genes Dev*, 25: 1628-40.